EGE UNIVERSITY

GRADUATE SCHOOL OF APPLIED AND NATURAL SCIENCES

(MASTER OF SCIENCE (MSc) THESIS)

EFFECTS OF ZINC OXIDE NANO PARTICLES ON ANTIBACTERIAL AND UV STABILIZING EFFECTS OF WOOD COATINGS

Övül KAYAALP

Supervised by: Prof. Dr. Sümer PEKER

Chemical Engineering

Discipline Code: 603.01.00
Date of Presentation: 28.05.2012

Bornova – İZMİR
2012

Övül KAYAALP tarafından Yüksek Lisans tezi olarak sunulan "**Effects of Zinc Oxide Nano Particles on Antibacterial and UV Stabilizing Effects of Wood Coatings**" başlıklı bu çalışma E.Ü. Lisansüstü Eğitim ve Öğretim Yönetmeliği ile E.Ü. Fen Bilimleri Enstitüsü Eğitim ve Öğretim Yönergesi'nin ilgili hükümleri uyarınca tarafımızdan değerlendirilerek savunmaya değer bulunmuş ve 28-05-2012 tarihinde yapılan tez savunma sınavında aday oybirliği/oyçokluğu ile başarılı bulunmuştur.

Jüri Üyeleri:		**İmza**
Jüri Başkanı	**: Prof.Dr. Sümer Peker**	.....
Raportör Üye	**: Prof.Dr. Şerife Helvacı**	.....
Üye	**: Prof.Dr.Hürriyet Polat**	.....

ÖZET

AHŞAP BOYALARINDA ÇİNKO OKSİT NANOTANELERİNİN ANTİBAKTERİYELLİK VE UV DAYANIMIÜZERİNE ETKİSİ

KAYAALP, Övül

Yüksek Lisans Tezi, Kimya Mühendisliği Anabilim Dalı
Tez Yöneticisi: Prof. Dr. Sümer PEKER
Temmuz 2012, 63 sayfa

Bu çalışmanın amacı, ahşap boyalarında çinko oksit nano tanelerinin, UV dayanımı ve antibakteriyellik üzerine etkisinin incelenmesidir.

Hidrotermal metod ile farklı morfolojilerde çinko oksit nanotaneleri üretilmiştir. Üretilen nano taneler, akrilik vernik içerisinde dağıtılmıştır. Dispersiyon koşulları, MERCK'in çinko oksit taneleri ile yapılan optimizasyon çalışması ile belirlenmiştir. Bu çalışmaya göre ZnO oranı %0.5, karıştırma hızı 2000 devir/dakika ve karıştırma süresi 30 dakika olarak tespit edilmiştir. Bu şartlara göre dispersiyonu sağlanan çinko oksit nano tanelerinin UV direncinin tespiti için akrilik vernik, siyah boya ile kaplanmış cam üzerine 90 mikron uygulanmıştır. Uygulanan yüzeyler üzerine UV dayanım testi yapılmıştır. Bu test ile UV ışığı altında vernikteki renk değişimi incelenmiştir. Bu renk değişimleri, üretilen çinko oksit nano tanelerinin morfolojik özellikleri ve optik özellikleri ile ilişkilendirilmiştir.

Çinko oksit nano tanelerinin, UV ışığını absorbe ederek, verniğin içerisindeki organik malzemelerin UV ışığı ile bozunmasını önlediği tespit edilmiştir. Yaprak lifler halinde oluşan çinko oksit nano tanelerinin, çubuk ve çiçek şeklinde oluşan nano tanelerine göre sararma direncini artırdığı da tespit edilmiş, bu çalışma ile morfolojinin etkisi açıkça görülmüştür.

Anahtar sözcükler: Ahşap boyaları, UV dayanım, çinko oksit nano taneleri, hidrotermal metod.

ABSTRACT

EFFECTS OF ZINC OXIDE NANO PARTICLES ON ACTIBACTERIAL AND UV STABILIZING EFFECTS OF WOOD COATINGS

KAYAALP, Övül

MSc in Chemical Engineering
Supervisor: Prof. Dr. Sümer PEKER
July 2012, 63 pages

The aim of this thesis is investigating the effect of zinc oxide nanoparticles on UV stabilizing and antibacterial effects of wood coatings.

Zinc oxide nano particles which have different morphologies are produced by hydrothermal method. Synthesized nanoparticles are dispersed into acrylic varnish. The dispersion conditions are determined with MERCK's zinc oxide by optimization work. According to optimization study, ratio of ZnO, impeller speed and mixing time are decided as 0.5%, 2000 rpm and 30 minutes, respectively. Acrylic varnish is applied on glass coated with black lacquer to investigate the effect of zinc oxide nanoparticles on UV stabilizing effect.After application, UV test is done. The color change of acrylic varnish under UV lights is observed with UV test. The morphologies and optical properties of ZnO nanoparticles are associated with the color change.

Zinc oxide nanoparticles absorb the UV lights and prevent the decomposition of organic compounds in acrylic varnish. The UV stability effect of nanosheets is better than rods and flower-like structures. The morphological effect on UV stability test is occured clearly in this thesis work.

Keywords: Wood coatings, UV resistant, zinc oxide nanoparticles, hydrothermal method.

ACKNOWLEDGEMENT

I wish to thank my supervisor, Prof. Dr. Sümer Peker for her valuable help and guidance throught this study.

I would like to thank to Prof. Dr. Şerife Helvacı for her help and support.

I would like to thank to Berrin İkizler for her support during the experiments.

I also thank to my family for their support and patience.

The thesis is financially supported by the fund of Scientific Research Project of Ege University with the project number of 10-MÜH-021.

TABLE OF CONTENTS

Page

TABLE OF CONTENTS (continued)

Page

LIST OF FIGURES

Figures **Page**

LIST OF TABLES

Tables **Page**

LIST OF TABLES (continued)

Tables **Page**

1. INTRODUCTION

Wood consists of three types of organic components: carbohydrates, lignin and extractives. Carbohydrates are polymers of sugars and make up 55% to 70% of wood. Approximately 20% to 30% of wood is composed of lignin that is a polymer. It helps bond cells together. Extractives is 1-3% of wood.

Carbohydrates do not absorb UV radiation. Therefore, it has UV resistivity. If wood is exposed to UV radiation, lignin begins to degrade within a few hours. Extractives change color when exposed to UV radiation. The color change causes wood to lighten or darken. [Williams, 2009]

Wood coatings are used on wooden surfaces such as veneer, MDF (medium density fiberboard), chipboard, massive to give an aesthetic aspect and protect the surface from outdoor conditions. Wood coatings are classified into two groups: transparent varnishes and pigmented lacquers.

Varnishes do not contain any pigment and they are transparent. Veneer surfaces are coated by varnish to be protected from outdoor conditions such as mechanical abrasion, UV radiation, household chemical attacks. Wood veneer is made from the wood of various species of trees. Altough, pigmented lacquers are applied on MDF surfaces.

Acrylic varnish used in this work is a two component system. It means that the curing of the varnish takes place with the help of a second component called ‘hardener’. The main component of the varnish is resin, a kind of polymer. The resin has hydroxyl functional groups that react with isocyanate functional groups of the hardener. The other varnish component is the catalyst. It initiates the reaction between hydroxyl group [OH^-] and isocyanate functional group [–N=C=O]. The reaction mechanism is given in Figure 1.1. Also, butyl acetate and methoxy propyl acetate are used as diluting agents to decrease the viscosity of varnish.

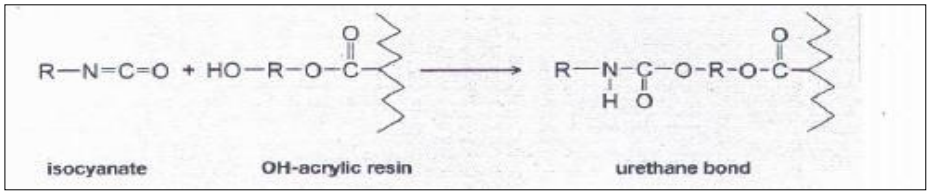

Figure 1.1 Reaction of isocyanates functional groups with hydroxygroups

Varnish or lacquer exposed to direct sunlight is damaged by UV radiation, that diffuses freely through the coating and destroys the organic compounds such as pigments, binders or polymers in the coatings.

UV radiation is in the wavelength range of 295 – 400 nm. Since the energy of radiation varies inversely with the wavelength, UV radiation has higher energy than sunlight. Because of its high energy content, it is capable of degrading macromolecular materials such as wood and also coatings by radical formation. Some of radicals form new bonds. In conjuction with the shortened chains this means a loss of mechanical strength and a reduction in elasticity at the same time. Poor cohesion and brittleness are the consequences. Supplementary changes in the color of the substrate, such as in wood, are also attributable to photochemical reactions. Such damage only occurs in the substrate if the high energy radiation is able to penetrate through the coating as far as the substrate. This is only the case, however, if the pigments or film forming agents are incapable of UV absorption [Goldschmidt, 2007].

Varnishes and lacquers exposed to sun light have to gain resistance to UV radiation by the addition of UV protection agents. These agents are divided into two groups: organic and inorganic absorbers. Conventional organic UV absorbers degrade over time with the effect of the sunlight and lose their efficiency. However, inorganic UV absorbers remain stable and provide long-lasting protection.The conventional organic UV absorber is HALS (hindered amine light stabilizer). The inorganic UV absorbers are oxides of metals such as zinc oxide and titanium dioxide.

Zinc oxide has been used in numerous applications, such as anti-reflection coatings, transparent electrodes in solar cells, varistors, light emitting diodes, gas sensors, acousto-optical devices, lasers, near-UV emissions, photocatalysis, antibacterial agents and piezoelectricdevices.

Various kinds of morphologies of ZnO including; nanopins, nanorods, nanotubes, nanoscrews, nanowhisker, obelisk-like, tower-like, flower-like and nanopencils have been produced. Since different morphologies of ZnO show different electron emission, optical, electrical and a coustic properties, many efforts have been carried out to find the optimum fabrication process for ZnO with excellent properties.

Zinc oxide forms electron-hole pairs under the influence of UV radiation (approx. 380 nm),when a photon collides with the electron; the high energy electron jumps from the valence band to the conduction band leaving a hole in the electronic shell. These electron-hole pairs recombine when the excited electron returns to its initial ground state energy with release of heat. On the metal oxide particle surface, the reactions take place with the formation of radicals. With water, the electron hole (h^+) reacts with OH^- to form reactive hydroxyl radicals. With atmospheric oxygen, the stimulated electron (e^-) responds to the oxygen superoxide radicals. These radicals oxidize organic bonds and attack bio-organisms. Organic molecules can also be adsorbed directly on the ZnO and be degraded by the redox process. Ideally, organic contaminations are split into CO_2 and water [Sepeur et al,2008]. The mechanism is given in Figure 1.2.

$$ZnO + UV\ light \rightarrow e^- + hole^+ \quad \text{(a)}$$

$$e^- + hole^+ \rightarrow ZnO + heat \quad \text{(b)}$$

$$hole^+ + OH^- \rightarrow OH^{\cdot} \quad \text{(c)}$$

$$e^- + O_2 \rightarrow O_2^{\cdot} \quad \text{(d)}$$

$$O_2^{\cdot} + OH^{\cdot} + (-CH_2-) \rightarrow intermediates \quad \text{(e)}$$

$$O_2^{\cdot} + OH^{\cdot} + intermediates \rightarrow CO_2 + H_2O \quad \text{(f)}$$

$$UV\ light + O_2 + (-CH_2-) \rightarrow intermediates \quad \text{(g)}$$

$$UV\ light + intermediates \rightarrow CO_2 + H_2O \quad \text{(h)}$$

Figure 1.2 UV protection mechanism of zinc oxide

In the literature, different morphologies of ZnO are obtained by using various methods. The characterization and optical analysis are done to investigate the synthesized ZnO nanoparticles. The summary of the literature that describes the formation of ZnO nanoparticles with different morphologies are given below as a guideline.

Ni, et. al. [2005] obtained rod-like ZnO nanoparticles with a band gap of 3.41 eV by the hydrothermal method. Fan, et. al.[2006] obtained ZnO rods with hexagonal structure by the hydrothermal method. The effects of the amount of NaOH used in production on optical properties of ZnO nanoparticles were investigated in this work. Flower-like ZnO morphology with different shapes by the hydrothermal method were produced in the work of Movahedi, et. al. [2008]. Wen, et. al. [2010] obtained ZnO whiskers by the hydrothermal method. In this work, the pH effect on morphology was investigated. ZnO whiskers with low aspect ratio were produced by increasing the solution pH. Nest-like ZnO nanoparticles were obtained in the work of Yan, et. al. [2009]. In this work, ZnO crystal has a wurtzite structure with UV emission at about 395 nm. Hajry, et. al. [2009] obtained hexaganol shaped ZnO rods by low temperature solution process. Flower-like and needle-like morphologies were obtained in the work of Xie et. al. [2009]. In this work, the effect of Zn^{2+}/OH molar ratio on morphology was investigated. Rod, needle, rugby and flower like structures were obtained by changing the reaction conditions in the work of Xie et. al. [2009]. The photocatalytic activity of ZnO particles were observed as a function of morphology. ZnO nanosheets were obtained with a band gap 3.39eV by simple-solution process at low temperature in the work of Umar, et. al. [2011].

The UV protection ability of ZnO particles were also investigated in the literature. The morphology of the ZnO particles were not an issue in these experiments.

As the effect of morphology on the UV protection is not investigated in the literature, the effect of the morphology on the effectiveness of the UV protection of the ZnO nanoparticles was the aim of this thesis project. New methods for obtaining ZnO nanoparticles with different morphologies were not included within the scope of this thesis work. Instead, the literature was searched for the methods of production of ZnO particles with different morphologies. These methods were adopted directly. In some cases, parametric investigations were done on these adopted methods.

2. EXPERIMENTAL

2.1 Materials and Methods

2.1.1 Materials

Zinc Nitrate: Zinc nitrate is in the form of $Zn(NO_3)_2.6\,H_2O$ and analytical grade purchased from MERCK. Its molecular weight is 297.46g/mol. It is used as the source of Zn^{2+} in the experiments to synthesize ZnO nanoparticles. 0.5 M of zinc nitrate solution is prepared in a 250mL volumetric flask. This solution is used in all experiments.

Zinc Sulphate: Zinc sulphate is in the form of $ZnSO_4.7H_2O$and analytical grade purchased from RIEDEL. Its molecular weight is 287.54g/mol. It is used as the source of Zn^{2+} ions in the experiments to synthesize ZnO nanoparticles. 0.2M of zinc sulphate solution is prepared in a 50mL volumetric flask. This solution is used in all experiments.

Zinc Chloride: Zinc chloride is in the form of $ZnCl_2$ and analytical grade purchased from MERCK. Its molecular weight is 136.28g/mol. It is used as the source of Zn^{2+} ions in the experiments to synthesize ZnO nanoparticles. 1M of zinc chloride solution is prepared in a 100mL volumetric flask. This solution is used in all experiments.

Sodium Hydroxide: Sodium Hydroxide is in the form of NaOH and analytical grade purchased from MERCK. Its molecular weight is 40.00g/mol. It is used as the source of OH^- ions in the experiments to synthesize ZnO nanoparticles. 1M and 4M of its solutions are prepared in a 500mL and 100mL volumetric flasks, respectively. These solutions are used in all experiments.

Ethylene Glycol: Ethylene Glycol is in the form of $C_2H_6O_2$ and analytical grade purchased. Its molecular weight is 62.07g/mol. It is used as the reaction medium in the experiments to synthesize ZnO nanoparticles. 30mL and 60mL of pure ethylene glycol are used in all experiments.

Ethanol: Ethanol is in the form of C_2H_5OH and analytical grade purchased from MERCK. The denstiy of ethanol is 0.79g/mL and its molecular weight is

46.07g/mol. It is used as the reaction medium in the experiments to synthesize ZnO nanoparticles. 30mL and 60mL of pure ethanol are used in all experiments.

Water: Distilled water is used in all experiments with a conductivity and pH value of 1.7μS/cm and 5.58, respectively.

SDS (Sodium Dodecyl Sulfate): SDS is in the form of $C_{12}H_{25}OSO_3Na$ and has a purity of greater than 99.00% (FLUKA). It is an anionic surfactant and used as a reaction medium in the experiments to synthesize ZnO nanoparticles. Its molecular weight is 288.38g/mol. 0.2M of its solution is prepared in a 50mL volumetric flask. This solution is used in the experiments.

Ammonia: An aqueous ammonia solution consisting of 25% ammonia is used without further purification. It is purchased from MERCK. The density of ammonia is 0.91g/mL and its molecular weight is 17.03g/mol. 0.2M of its solution is prepared in a 100mL volumetric flask. This solution is used in the experiments.

Zinc Oxide: Zinc oxide is in the form of ZnO and has a purity of 99% (MERCK). Its molecular weight is 81.39g/mol. It is used for optimization works to determine the best dispersion conditions for the experiments.

Acrylic Varnish: Acrylic varnish used in experiments consists of short oil alkyd, butyl acetate, catalyst and methoxy propyl acetate.

Short oil alkyd is a resin of acrylic varnish. Resin is the most important component that gives all properties to varnish film such as hardness, drying, protecting the wood. It has hydroxyl polymer groups [OH-]. These groups react with [–N=C=O] groups that come from hardener.

Catalyst is the used in the formulation to initiate the reaction between the hydroxyl polymer groups and [–N=C=O] groups. Butyl acetate and methoxy propyl acetate are used in the formulation to dilute the varnish.

Hardener: Hardener is an isocyanate with the [–N=C=O] groups used for curing of acrylic varnish. 50g of hardener is added in the 100g of acrylic varnish to provide curing.

2.1.2 Methods

2.1.1.1 Instruments used

Measurement of Weight: The required amounts of species and samples are weighed by using the Sartorious GP603-S scale.

Mixing of Solutions: The samples and species are mixed by IKA-Labortechnik RH basic magnetic stirrer and also with IKA-Werke mechanical stirrer.

Drying of Equipment: The all glassware are dried by NUVE KD 200 drying oven at 60-70^{o}C for 24h.

Measurement of pH: pH is measured with a WTW PH 330/SET-1.

Investigation of Crystal Structure: Crystal Structure of ZnO is determined with Phillips X'Pert Pro X-Ray Diffractometer (XRD) a scanning rate of 4 deg/min in a 2θ range from 0^{o} to 80^{0}.

Appearence of ZnO Nanoparticles: Images obtained in Scanning Electron Microscopy (SEM), Phillips XL-30S are used to observe the particle shape of materials.

Measurement of Color Difference: X-Rite spectrophotometer is used to determine the color change after UV test.

Optical Characterization of ZnO Nanoparticles: The diffuse reflectance spectra of nanoparticles are measured using Shimadzu UV-2600-ISR UV/Vis spectrophotometer with integrating sphere attachment (λ=200-800nm).

UV Stabilization Test: Cefla UV2000 UV lamps are used for UV stabilizing test.

2.1.1.2 Methods of production of zinc oxide nanoparticles

ZnO nanoparticles are synthesized by several methods such as; solvothermal synthesis, sol-gel method, microemulsion method, thermal hydrolysis, hydrothermal synthesis.

Among the synthesis methods, the hydrothermal method is the most attractive one due to its perfect control of morphology, purity, crystallinty, composition and low cost for large-scale production.

Hydrothermal processing can be defined as any heterogeneous reaction in the presence of aqueous solvents or mineralizers under high pressure and temperature conditions to dissolve and recrystallize materials that are relatively insoluble under ordinary conditions.

Zn sources along with different mineralizers and additives are used in hydrothermal method. The experiments can be carried out within a temperature range, 100 – 250^{o}C. The Zn source, solvent, pH, experimental temperature and the additives control the size and shape of the particles.

The selection of zinc salts and reactants are important factors in the production of ZnO powder. Zinc nitrate ($Zn(NO_3)_2$), zinc sulfate ($ZnSO_4$) and zinc chloride ($ZnCl_2$) are the possible zinc salts that can be used as a Zn^{2+} source. NaOH is added to Zn^{2+} solution to obtain a higly basic solution. Most frequently used reactant is sodium hydroxide (NaOH) such as the source of OH^-. The only stable form can exist in highly basic (pH = 13-14).

NaOH solution is added into the solution of zinc salts. The first step of the reaction is $Zn(OH)_2$ precipitate formation.

$$Zn^{2+}_{(aq)} + 2OH^-_{(aq)} \Leftrightarrow Zn(OH)_{2(s)} \quad (2.1)$$

Continue to add NaOH solution, $Zn(OH)_{2(s)}$ dissolves and yield clear precursor solution which is in the form of $Zn(OH)^{2-}_{4(aq)}$. Upon heating of the precursor solution, ZnO particles are obtained.

$$Zn^{2+}_{(aq)} + 4OH^-_{(aq)} \Leftrightarrow Zn(OH)^{2-}_{4(aq)} \quad (2.2)$$

$$Zn(OH)_{4(aq)}^{2-} \xrightarrow{\Delta} ZnO_{(s)} + H_2O_{(l)} + 2OH^- \quad (2.3)$$

The details of the various procedures for obtaining different morphologies are given below.

Experiment 1: Zinc nitrate hexahydrate ($Zn(NO_3)_2.6\,H_2O$) and sodium hydroxide (NaOH) are used as the source of Zn^{2+} and OH^-, respectively. 1M solution of NaOH with the volume of 100mL is placed in a glassware. 0.5M solution of $Zn(NO_3)_2.6\,H_2O$ with the volume of 10mL is added onto NaOH solution to obtain the precursor solution. 30mL of this solution is put into aoutoclave. Solvent as a reaction medium is added onto the precursor solution to control the formation of zinc oxide. The reaction takes place at 160^{o}C [Xiao, 2008].

Experiment 2: The method of Gusatti [2008] is obtained nanorods by low reaction temperature. Zinc nitrate hexahydrate ($Zn(NO_3)_2.6\,H_2O$) and sodium hydroxide (NaOH) are used as the source of Zn^{2+} and OH^-, respectively. 1M of NaOH solution is prepared by weighing 20g of NaOH in 500mL pure water. 0.5M of $Zn(NO_3)_2.6\,H_2O$ solution is prepared by weighing 37.1825g of $Zn(NO_3)_2.6\,H_2O$ in 250mL pure water. 100mL of NaOH solution is placed in a glassware and heated up to 70^{o}C. 100 mL $Zn(NO_3)_2.6\,H_2O$ solution is added into NaOH solution under vigorous stirring at 70^{o}C. The resultant solution is kept stirred for two hours after the solution is maintained in 70^{o}C.

Experiment 3: The reaction conditions are the same with Experiment 2. The ratio of $[OH^-]/[Zn^{2+}]$ is changed to obtain different morphologies. The molar ratio of Experiment 3 is 6 that is greater three times than the molar ratio of Experiment 2.

Experiment 4: ZnO balls made of nanosheets are obtained in the method of Umar [2011]. In this experiment, this method is investigated. Zinc nitrate solution ($Zn(NO_3)_2.6\,H_2O$) and sodium hydroxide solution (NaOH) was used in the experiment. 80 mL of 0.5 M $Zn(NO_3)_2.6\,H_2O$ is put in a glassware. 120 mL of 1M NaOH solution is added into zinc nitrate solution to adjust the pH to 12.83. The resultant solution is stirred by magnetic stirrer for 30 minutes at room temperature (20 – 25^{o}C) and 6 hours at 90^{o}C.

Experiment 5: The method of Usui [2009] is investigated in this experiment. Sodium dodecyl sulfate (SDS), hexamethylenetetramine (HMT), cetyltrimethylammonium bromide (CTAB) are used as additive in the reactions to investigate the effect on morphologies by Usui [2009]. In this experiment, NH_3 solution is used as additive to obtain ZnO nanoparticles. Zinc sulfate ($(ZnSO_4).7H_2O$) and sodium hydroxide (NaOH) are used as the source of Zn^{2+} and OH^-, respectively.0.2M zinc sulfate solution and 4M NaOH solution is prepared in 100mL volumetric flask by weighing 5.751g and 16g, respectively. 50mL of zinc sulfate solution is put into a glassware. NaOH solution is added into zinc nitrate solution to adjust pH to 12 -13. 10mL of NaOH solution is needed to set the pH at 12.80. An aqueous ammonia solution consisting of 25% ammonia is used as additive to control the morphology of ZnO powder. 0.2M NH_4OH solution is prepared by taking 1.5mL of ammonia solution and filled up to 100mL with distilled water. 50mL of NH_3 solution is added into precursor solution. The resultant solution is stirred at 5°C for 1 hour and at room temperature (20-25°C) for 1.5 hours. Then the resultant solution is put into aoutoclave at 90°C for 5 hours.

Experiment 6: The reaction conditions are the same with Experiment 5. The difference is only the additive used to obtain different morphology of ZnO powder. Sodium dodecyl sulfate (SDS) solution is used as additive to control the morphology of ZnO powder [Usui, 2009].

Experiment 7: The method of Li et.al. [2008] investigate the reaction temperature effect on the ZnO morphology. In this experiment, zinc chloride ($ZnCl_2$) and sodium hydroxide (NaOH) are used as the source of Zn^{2+} and OH^-, respectively. 1M zinc chloride solution and 4M NaOH solution is prepared in 100mL volumetric flask by weighing 13.628g and 16g, respectively. Sodium dodecyl sulfate (SDS) solution is used as additive to control the morphology of ZnO powder. 30mL of 4M NaOH solution and 5 mL of 0.2M SDS solution are added onto 20mL of 1 M $ZnCl_2$ solution. Then, the resultant solution is diluted with 45mL of distilled water under vigorous stirring at 5^oC. After adding the distilled water, the solution is stirred at room temperature (20-25°C) for 2 hours. Finally, the solution is put into an aoutoclave at 85°C for 5 hours.

Experiment 8: In this experiment, Experiment 7 is repeated without stirring at room temperature to investigate the effect of this step on the morphology of

ZnO nanoparticles. The other conditions of reaction are the same with Experiment 7.

The summary of reaction conditions and expected morphologies of Experiments 2 to 8 are given in Table 2.1. Flowers, nanosheets, rods, 3D rods (flowers formed by long rods) are expected morphologies according to literature surveys.

Table 2.1 The summary of reaction conditions of Experiments 2 to 8

Exp No	Zn^{2+} salt	Add.	$\frac{[OH^-]}{[Zn^{2+}]}$	Reaction Conditions		Reference	Expected Morphology
				Rxn. Temp.	Rxn. Time		
2	$Zn(NO_3)_2$	-	2	70°C	2 h	Gusatti,2008	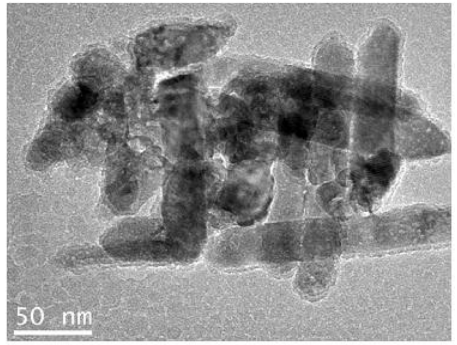
3	$Zn(NO_3)_2$	-	6	70°C	2 h	Gusatti,2008	-
4	$Zn(NO_3)_2$	-	3	20°C 90°C	30 min. 6 h	Umar,2011	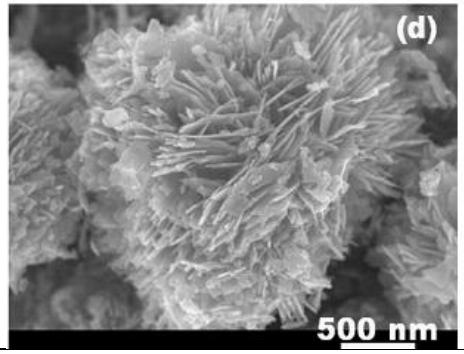

Table 2.1 (continued) The summary of reaction conditions of Experiments 2 to 8

Exp No	Zn^{2+} salt	Add.	$\frac{[OH^-]}{[Zn^{2+}]}$	Reaction Conditions		Reference	Expected Morphology
				Rxn. Temp.	Rxn. Time		
5	$ZnSO_4$	NH_3	4	5°C 20°C 90°C	1 h 1.5 h 5 h	Usui,2009	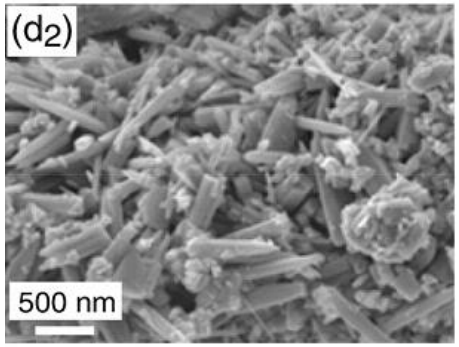 * CTAB is used as an additive in the method of Usui,2009
6	$ZnSO_4$	SDS	4	5°C 20°C 90°C	1 h 1.5 h 5 h	Usui,2009	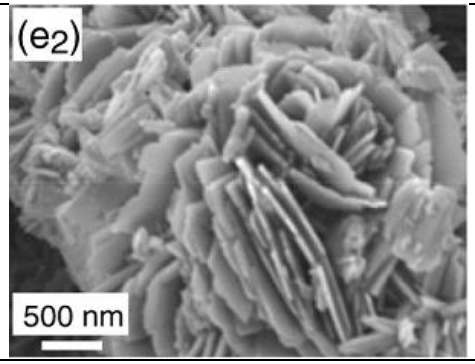

Table 2.1 (continued) The summary of reaction conditions of Experiments 2 to 8

Exp No	Zn^{2+} salt	Add.	$\frac{[OH^-]}{[Zn^{2+}]}$	Reaction Conditions		Reference	Expected Morphology
				Rxn. Temp.	Rxn. Time		
7	$ZnCl_2$	SDS	6	5°C 25°C 90°C	3 min. 2 h 5 h	Li,2008	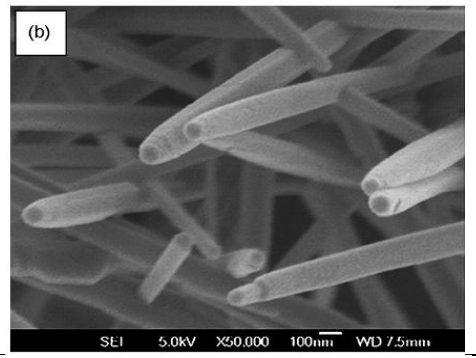
8	ZnCl2	SDS	6	5°C 90°C	3 min. 5 h	Li,2008	

2.2 Optimization of Dispersion Conditions of ZnO Nanoparticles in Varnish

Merck's ZnO powder is used to determine the optimum amount of ZnO into coating to provide UV resistance. Also, impeller speed and mixing time is obtained for effective dispersion of ZnO nano particles into coating.

Two different amounts of ZnO (0.5-1.5%, by weight), three different impeller speed (1000-1500-2000 rpm) and three different mixing time (10-20-30 min.) are studied for optimization.

Acrylic varnish is used for optimization studies. 75g acrylic varnish weighed is placed in a metallic cup. In the first run, 0.5% ZnO is used and added onto varnish by weighing 0.375g. The sample is repeated 9 times. Each sample is mixed by a magnetic stirrer at 1000-1500-2000 rpm for 10-20-30 minutes, respectively. At the second run, 1.5% ZnO is used and added onto varnish by weighing 1.125g. The same process at the first run is repeated in the second run. After dispersion for all set, the varnish is kept a side for 5 minutes for foams formed during stirring to break up. Then 37.5g hardener was added in the varnish. Then the mixture is applied on a glass by an applicator. The film thickness of mixture is 90μ.

2.3 Preparation of Acrylic Varnish with ZnO Powders

ZnO powders synthesized by experiments are dispersed into acrylic varnish by using mechanical stirrer. According to optimization studies, the weight percentage of ZnO powder in the varnish is decided as 0.5%. 100g of acrylic varnish is placed in a metallic cup. 0.5g of ZnO powder is weighed and added into varnish. ZnO powder is dispersed for 30 minutes at 2000 rpm. After dispersion, the varnish is waited for 5 minutes to prevent foams formed during stirring. Then 50 gr hardener is added in the varnish. Then the mixture is applied on a glass by applicator. The film thickness is 90μ.

2.4 Dispersion Behaviour of ZnO Powder in the Solvent

Dispersion is an important factor in the reflection of UV light. Homogenous dispersion is aimed. The morphology of particles in varnish after dispersion can not be observed due to gel formation in the varnish. Therefore, ZnO nanoparticles

synthesized are dispersed in the solvent, butyl acetate for 30 minutes at 2000 rpm. After dispersion, a few drops put on the carbon black tape. Butyl acetate evaporates and ZnO nanoparticles are left on the tape. SEM images are investigated easily without gel formation. The extend of dispersion of the particles with different morphologies could be observed.

2.5 UV Stabilizing Test

ZnO powders synthesized are dispersed in acrylic varnish to determine UV stabilizing effect. Varnish is applied on a glass which is painted with black top coat. Applicator is used to apply the varnish on the glass. The glass on which acrylic varnish is applied and applicator are shown in Figure 2.1

a) Applicator

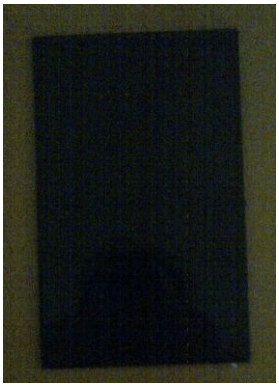

b) Glass

Figure 2.1 The images of (a) applicator and (b) glass

The varnish applied on the glass should be cured completely for UV test. So, the varnish is waited at least one week for UV stabilizing test. Half of the glasses was covered with paper. Then they are exposed to UV light by special UV lamps. High-pressure mercury lamps are used for UV test. The high-pressure mercury lamp emits ultraviolet radiation in the UVA band. The wavelength of the mercury lamp is 365 nm.

The sun effect on the coating is simulated with this test. The sun emits the ultarviolet radiation in the UVA, UVB and UVC bands. But, observing the effects of UV lights from sun take a long time such as one week. Using UV lamps speed up the test.

2.6 Optical Characterization of ZnO Nanoparticles

Optical characterization is needed to show the performance of ZnO nanoparticles under UV radiation. Optical characterization of ZnO nanoparticles are done by Shimadzu UV-2600-ISR UV/Vis spectrophotometer. Reflectance of synthesized ZnO nanoparticles are measured. The wavelength at which the maximum reflectance starts is determined using the reflectance vs. wavelength plotting. Up to the morphologies of experiments, the differences between the wavelengths are investigated. However, band gap energy of the ZnO nanoparticles are determined by Kubelka-Munk function. The effect of morphology on reflectance and band gap energy is investigated and evaluated. Also, UV stabilizing effect of ZnO powders are associated with their reflectance values and band gap energies.

3. RESULTS AND DISCUSSION

3.1 Optimization Studies

To obtain the optimum amount of ZnO, impeller speed and stirring time, the optimization studies are conducted using ZnO (MERCK) and the parameters studied are summarized in Table 3.1.

Two different amounts of ZnO (0.5-1.5%, by weight), three different impeller speeds (1000-1500-2000 rpm) and three different mixing times (10-20-30 min.) are studied for optimization.

Table 3.1 Experiments done with ZnO (MERCK) for optimization

	Amount of ZnO (%)	**Impeller Speed (RPM)**	**Mixing Time (min.)**
1	0.5	1000	10
2			20
3			30
4		1500	10
5			20
6			30
7		2000	10
8			20
9			30
10	1.5	1000	10
11			20
12			30
13		1500	10
14			20
15			30
16		2000	10
17			20
18			30

Optimization conditions are decided after UV test results. The important point for the UV test is getting the minimum color change between the parts of varnish that expose and not expose UV lights. The color change of acrylic varnish after UV test are given in Table 3.2.

Table 3.2 The color change of acrylic varnish after UV stabilizing test

	L	**a**	**b**	**ΔL**	**Δa**	**Δb**	**ΔE**
Std.	2.40	0.10	0.40	0.00	0.00	0.00	0.00
Std*	1.90	0.10	0.30	-0.53	-0.03	-0.05	0.53
1	5.30	0.30	-1.50	2.91	0.18	-1.82	3.44
1*	4.80	0.60	-0.20	2.41	0.50	0.58	2.53
2	4.10	0.40	-1.20	1.67	0.24	-1.51	2.26
2*	5.80	0.80	0.40	3.43	0.72	0.07	3.50
3	3.70	0.20	-1.30	1.35	0.09	-1.61	2.10
3*	7.40	0.80	-0.90	4.97	0.70	-1.24	5.17
4	3.70	0.20	-1.20	1.33	0.11	-1.55	2.05
4*	4.90	0.40	-1.50	2.47	0.25	-1.87	3.11
5	3.90	0.03	-1.30	1.52	0.17	-1.68	2.27
5*	4.70	0.30	-1.70	2.34	0.23	-2.04	3.12
6	5.50	0.30	-2.40	3.12	0.15	-2.76	4.17
6*	6.20	0.30	-2.80	3.83	0.15	-3.18	4.98
7	5.50	0.50	-1.80	3.11	0.43	-2.13	3.79
7*	6.10	0.50	-2.20	3.67	0.40	-2.53	4.47

Table 3.2 (continued) The color change of acrylic varnish after UV stabilizing test

	L	**a**	**b**	**ΔL**	**Δa**	**Δb**	**ΔE**
8	5.80	0.50	-2.30	3.44	0.35	-2.65	4.36
8*	5.00	0.40	-1.70	2.65	0.25	-2.08	3.37
9	5.20	0.50	-1.25	2.76	0.41	-1.58	3.21
9*	4.80	0.20	-2.10	2.42	0.11	-2.45	3.45
10	13.20	0.90	-7.60	10.82	0.81	-7.97	13.47
10*	15.70	0.40	-7.40	13.30	0.25	-7.78	15.41
11	14.90	1.00	-8.30	13.54	0.88	-8.65	16.09
11*	14.90	0.40	-7.70	12.54	0.26	-8.09	14.92
12	16.20	0.80	-8.80	13.83	0.70	-9.20	16.63
12*	14.80	0.50	-8.10	12.45	0.38	-8.43	15.04
13	16.30	1.00	-8.20	13.90	0.90	-8.53	16.34
13*	18.90	0.20	-6.80	16.49	0.10	-7.17	17.98
14	14.50	0.80	-8.80	12.11	0.65	-9.16	15.19
14*	17.10	0.50	-9.00	14.75	0.43	-9.35	17.47
15	8.80	0.70	-6.00	6.40	0.58	-6.31	9.00
15*	9.90	0.40	-6.50	7.52	0.33	-6.82	10.16

Table 3.2 (continued) The color change of acrylic varnish after UV stabilizing test

	L	**a**	**b**	**ΔL**	**Δa**	**Δb**	**ΔE**
16	9.80	0.60	-6.00	4.73	0.44	-6.35	9.79
16*	9.70	0.40	-6.30	7.27	0.30	-6.61	9.83
17	9.60	0.60	-6.60	7.21	0.53	-6.92	10.01
17*	8.20	0.40	-5.70	5.75	0.29	-6.09	8.38
18	8.70	0.60	-6.20	6.29	0.51	-6.51	9.07
18*	10.30	0.40	-6.60	7.94	0.29	-6.92	10.54

*The color results of varnish exposed to UV light.

Δ represents the difference between standart and sample. The standart does not include ZnO nanoparticles. So, if standart exposed to UV light is compared with sample exposed to UV light, the UV stabilizing effect of ZnO can be observed.

If ΔL is positive, the sample is lighter than standart. If negative, it is darker than the standart.

If Δa is positive, the sample is more red then standart (or less green). If negative, the sample is more green (less red).

If Δb is positive, the sample is more yellow (or less blue). If negative, the sample is more blue (or less yellow). It is the most important value for UV test.

According to the color change given in Table 3.2, Δb is negative for all set of experiments. However, the using of efficient amount is important if homogenous dispersion and raw material costs are considered.

The optimization conditions are decided as the ZnO amount; %0.5, the impeller speed; 2000 rpm and mixing time; 30 minutes.

3.2 Characterization of ZnO Powders Synthesized

ZnO nanoparticles are characterized by scanning electron microscopy (SEM) for their morphological appearence; by X-ray diffraction analysis (XRD) for their crystal structure; and by UV spectrophotometer for their optical reflectance in the UV region.

3.2.1 SEM analysis

Synthesized ZnO powders are analysed with Scaning Electron Microscopy (SEM). The aim of this production is to get different morphologies of ZnO powders. For this reason, the reaction conditions are changed and investigated to observe the effects on morphology.

Some parameters which effect the morphology of ZnO are investigated in Experiment 1. Investigated parameters are given in Table 3.3.

Table 3.3 Investigated parameters in ZnO production using zinc nitrate hexahydrate at 160°C

Reaction	**$Zn(OH)_4^{2-}$ (mL)**	**Solvent (mL)**	**Solvent Type**	**Solvent / $Zn(OH)_4^{2-}$ (volume ratio)**	**Reaction Time (h)**
1	30	30	Water	1:1	2
2	30	30	Water	1:1	4
3	30	60	Water	2:1	2
4	30	60	Water	2:1	4
5	30	30	Ethylene Glycol	1:1	2
6	30	30	Ethylene Glycol	1:1	4
7	30	60	Ethylene Glycol	2:1	2
8	30	60	Ethylene Glycol	2:1	4
9	30	30	Ethanol	1:1	2

Table 3.3 (continued) Investigated parameters in ZnO production using zinc nitrate hexahydrate at 160°C

Reaction	**$Zn(OH)_4^{2-}$ (mL)**	**Solvent (mL)**	**Solvent Type**	**Solvent / $Zn(OH)_4^{2-}$ (volume ratio)**	**Reaction Time (h)**
10	30	30	Ethanol	1:1	4
11	30	60	Ethanol	2:1	2
12	30	60	Ethanol	2:1	4

SEM images of ZnO particles obtained by the reaction in Experiment 1 are given in Table 3.4. From SEM images, the structures of the ZnO nanoparticles can be seen clearly.

The morphology of the reaction 1 is flowers-like structures formed from aggregated rods. In reaction 2, flower-like structures formed from aggregated rods are observed which is the same as the structures obtained with reaction 1. The ends of the rods are linked and bone-like structures are formed in reaction 3. A lot of rods are aggregated and ball-like structures of dumb-bell shaped are formed in reaction 4. In this structure, two balls are connected with each other and distributed homogenously. In reaction 5 -7 - 8, the flower-like structures are formed, but these structures are different from the structure, of reaction 1. In reaction 6, the rods and flower-like structures are formed. This is the mixed-type structure. Cauliflower-like structures are formed in reaction 9 and 11. Flower-like structures formed aggregated of needle-like rods are formed in reaction 10. There is no structure in reaction 12.

The effect of three parameters on the morphology are investigated in the first experiment. The first parameter is the solvent type in which reaction takes place. The solvent used in the reactions as a reaction medium are water, ethylene glycol and ethanol, respectively. The second parameter is the ratio of solvent to precursor solution. The last parameter is the reaction time. Reactions take place in 2 hours and 4 hours, respectively. The reaction temperature is constant at 160^oC in all cases.

The effect of the solvent type on the morphology is investigated firstly. The reactions are divided into groups: the effect of the solvent, with the other parameters held constant is investigated in the first group (reactions 1-5-9). The

effect of the solvent is investigated as in the second group (reactions 2-6-10) with the reaction time longer than the first group of experiments. The mole ratio is changed in the third group (reactions 3-7-11) of experiments with all other conditions the same as the first group. The mole ratio of the second group of the experiments is increased in the fourth group (reactions 4-8-12). The difference is only the solvent type among the reactions within the groups. In the first group, the reaction time is held constant as 2 hours and the ratio of the solvent to precursor solution as, 1:1. In the second group, the reaction time is held constant as 4 hours and the ratio of the solvent to precursor solution as, 1:1. In the third group, the reaction time is again2 hours, but the ratio of the solvent to precursor solution is 2:1. In the last group, the reaction time is held constant as 4 hours and the ratio of the solvent to precursor solution, as 2:1.

Table 3.4 SEM images of Experiment 1

Solvent Type	Reaction No	Solvent / $Zn(OH)_4^{2-}$	Rxn Time,h	Scale of SEM Images		
WATER	1	1:1	2	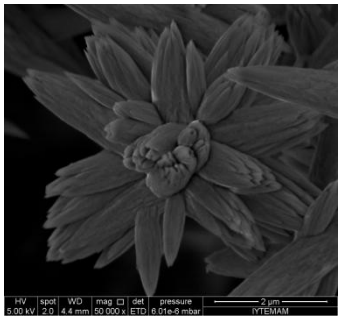		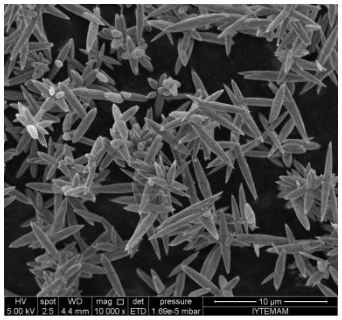
				50 000 X	20 000 X	10 000 X
	2	1:1	4	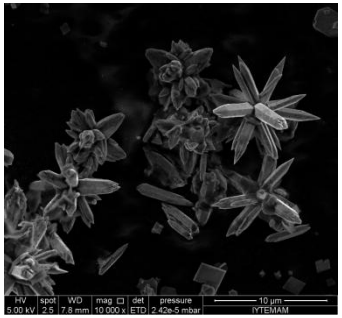	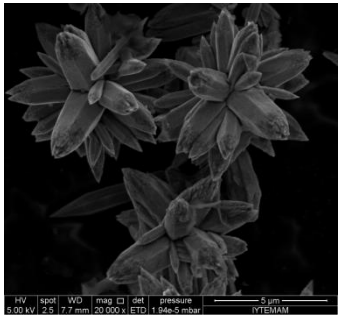	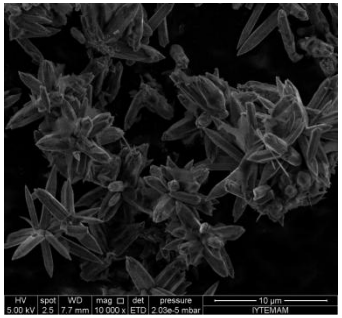
				50 000 X	20 000 X	10 000 X

Table 3.4 (continued) SEM images of Experiment 1

Solvent Type	Reaction No	Solvent / $Zn(OH)_4^{2-}$	Rxn Time,h	Scale of SEM Images		
WATER	3	2:1	2	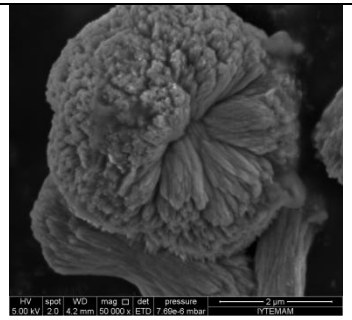	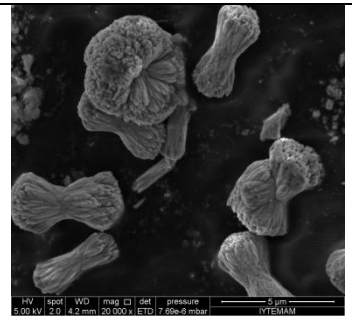	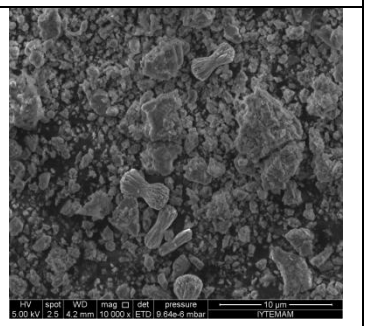
				50 000 X	20 000 X	10 000 X
	4	2:1	4		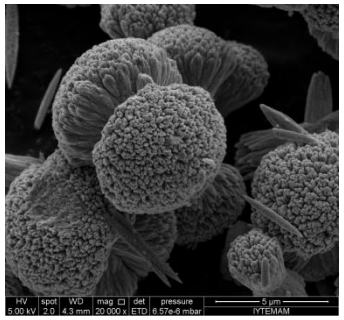	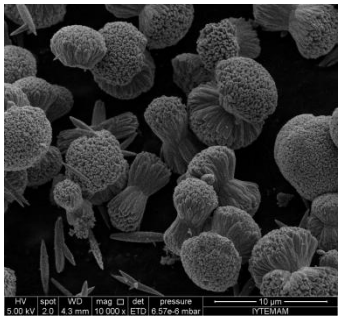
				50 000 X	20 000 X	10 000 X

Table3.4 (continued) SEM images of Experiment 1

Solvent Type	Reaction No	Solvent / $Zn(OH)_4^{2-}$	Rxn Time,h	Scale of SEM Images		
ETHYLENE GLYCOL	5	1:1	2	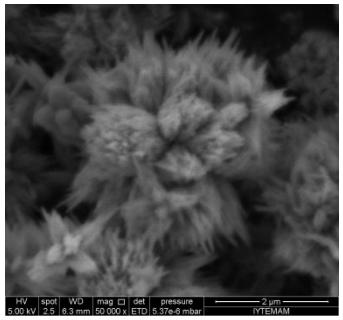	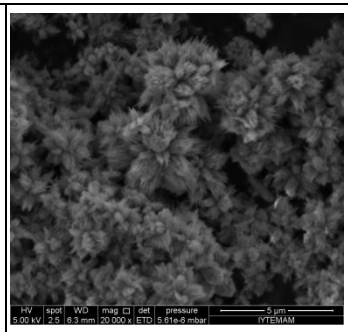	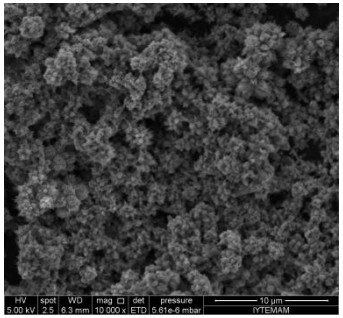
				50 000 X	20 000 X	10 000 X
	6	1:1	4	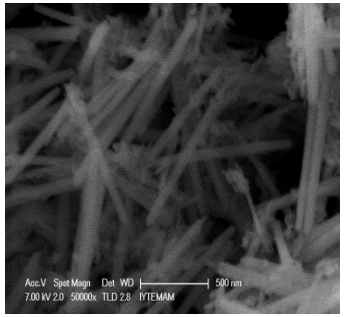	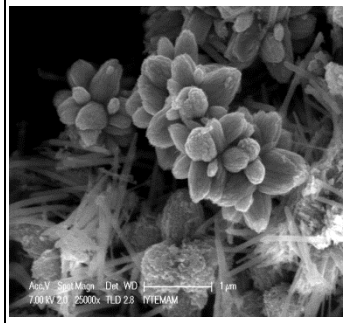	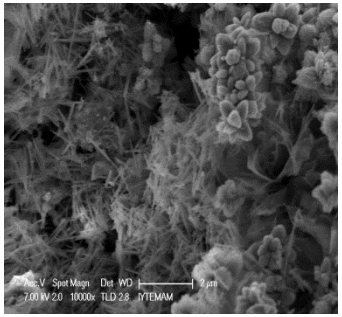
				50 000 X	20 000 X	10 000 X

Table 3.4 (continued) SEM images of Experiment 1

Solvent Type	Reaction No	Solvent / $Zn(OH)_4^{2-}$	Rxn Time,h	Scale of SEM Images		
ETHYLENE GLYCOL	7	2:1	2	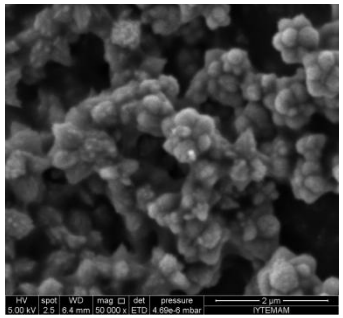	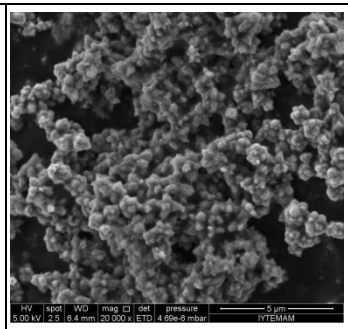	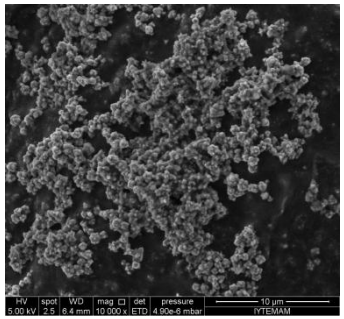
				50 000 X	20 000 X	10 000 X
	8	2:1	4	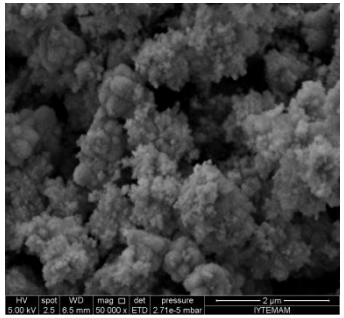	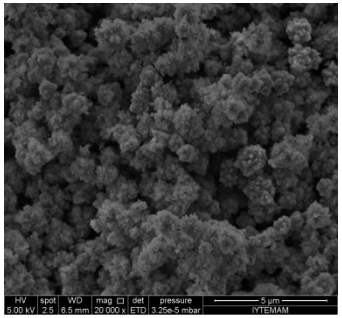	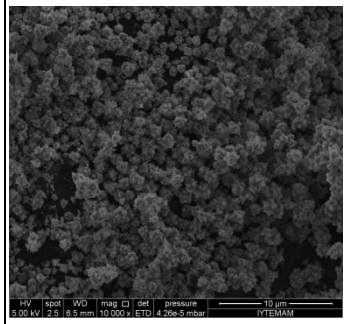
				50 000 X	20 000 X	10 000 X

Table 3.4 (continued) SEM images of Experiment 1

Solvent Type	**Reaction No**	**Solvent / $Zn(OH)_4^{2-}$**	**Rxn Time,h**	**Scale of SEM Images**		
ETHANOL	9	1:1	2	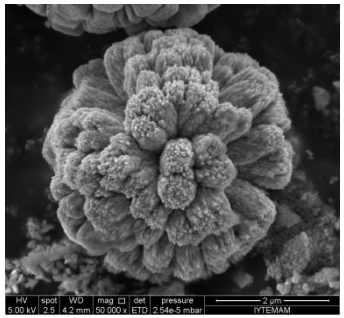	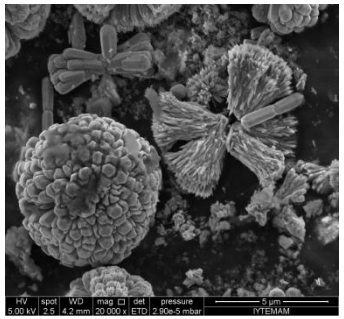	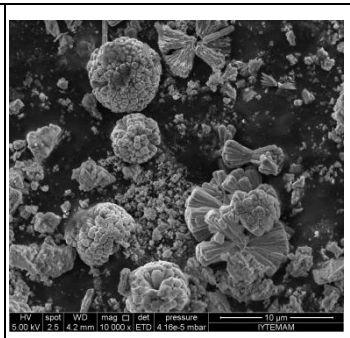
				50 000 X	20 000 X	10 000 X
	10	1:1	4	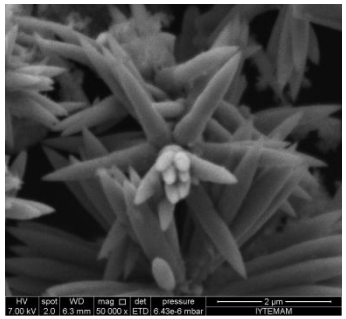	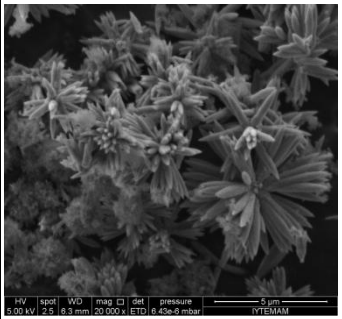	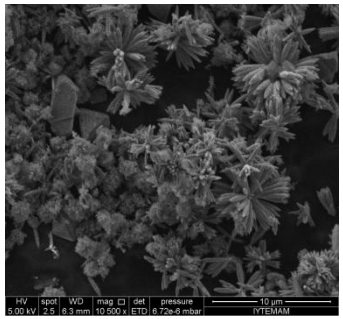
				50 000 X	20 000 X	10 000 X

Table 3.4 (continued) SEM images of Experiment 1

Solvent Type	**Reaction No**	**Solvent / $Zn(OH)_4^{2-}$**	**Rxn Time,h**	**Scale of SEM Images**		
ETHANOL	11	2:1	2	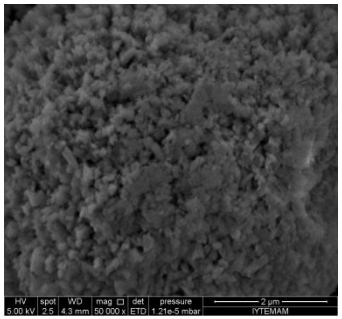	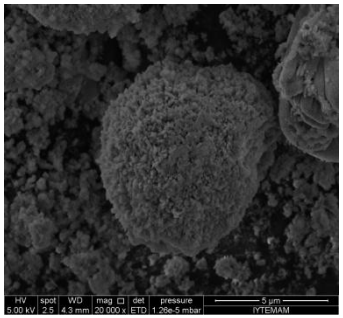	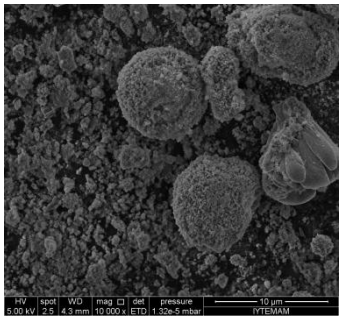
				50 000 X	20 000 X	10 000 X
	12	2:1	4	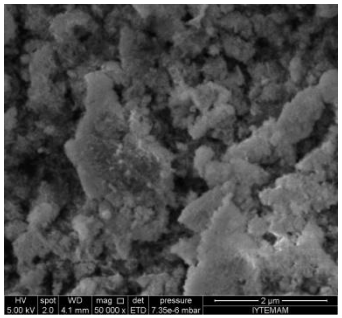	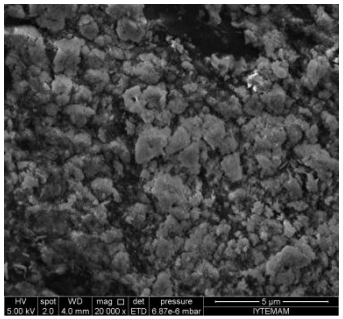	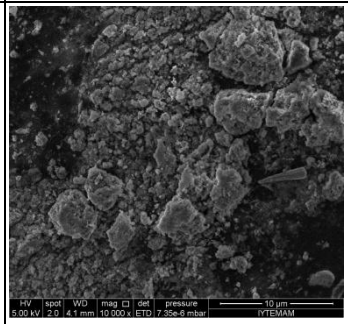
				50 000 X	20 000 X	10 000 X

The morphologies are compared according to solvent type and given in Table 3.5.

Table 3.5 The effects of solvent type on the morphology of ZnO for Experiment 1

Reaction Conditions	**Solvent Type**		
	Water	**Ethylene Glycol**	**Ethanol**
Reaction Time : 2h Solvent / $Zn(OH)_4^{2-}$: 1/1	Flower like structures formed by nano rods	Flower like structures formed by small particles	Cauliflower like structures
Reaction Time: 4h Solvent / $Zn(OH)_4^{2-}$:1/1	Flower like structures formed by nano rods	Flower like structures formed by small particles	Flower like structures formed by aggregation of needle-like rods
Reaction Time: 2h Solvent / $Zn(OH)_4^{2-}$:2/1	Ball-shaped structures	Rods and flower-like structures - mixed-type structure	Cauliflower like structures
Reaction Time: 4h Solvent / $Zn(OH)_4^{2-}$:2/1	Bone like structures formed by linking the ends of the rods	Flower like structures formed by small particles	No structures formed

The second and third investigated parameters are the ratio of solvent to precursor solution ($Zn(OH)_4^{2-}$) and time, respectively. The morphologies are compared and given in Table 3.6.

Table 3.6 The effects of solvent ratio and reaction time on the morphology of ZnO for Experiment 1

Reaction Conditions	**Reaction Time**	
	2 h	**4 h**
Reaction Solvent: Water Solvent / $Zn(OH)_4^{2-}$:1/1	Flower like structures formed by nano rods	Flower like structures formed by nano rods (smaller structures)
Reaction Solvent: Water Solvent / $Zn(OH)_4^{2-}$: 2/1	Ball-shaped structures	Bone like structures formed by linking the end of rods
Reaction Solvent: E. Glycol Solvent / $Zn(OH)_4^{2-}$: 1/1	Flower like structures formed by small particles	Rods and flower-like structures - mixed-type structure
Reaction Solvent : E. Glycol Solvent / $Zn(OH)_4^{2-}$: 2/1	Flower like structures formed by small particles	Flower like structures formed by small particles
Reaction Solvent: Ethanol Solvent / $Zn(OH)_4^{2-}$: 1/1	Cauliflower like structures	Flower like structures formed byaggregation of needle-like rods
Reaction Solvent: Ethanol Solvent / $Zn(OH)_4^{2-}$: 2/1	Cauliflower like structures	No structures formed

Different morphologies are obtained with Experiment 1. Also, the effect of solvent type, reaction time and solvent ratio on morphology are observed as summarized in Table 3.5 and Table 3.6, respectively. But, the disadvantage of Experiment 1 production can not be done on a large scale. Therefore, it is not suitable for industrial scale production.

Large-scale production is achieved with experiments given in Table 3.7. ZnO powders are synthesized under different reaction conditions to obtain different morphologies such as flowers, connected plates, plates with serrated edges, rods and connected rods (Table 3.7). Reaction time, reaction temperature, reaction medium, Zn^{2+} source and the molar ratio of $[OH^-]/[Zn^{2+}]$ are variables in Experiments 2 to 8.

Table 3.7 SEM images of Experiments 2 to 8

Exp. No	**Zn^{2+} salt**	**Additive**	**$\frac{[OH^-]}{[Zn^{2+}]}$**	**Reaction Conditions**	**Scale of SEM Images**		
2	$Zn(NO_3)_2$	-	2	70°C; 2 h	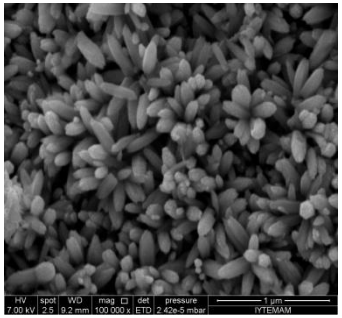	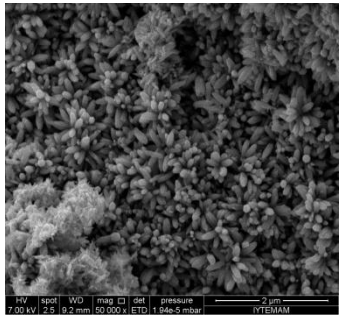	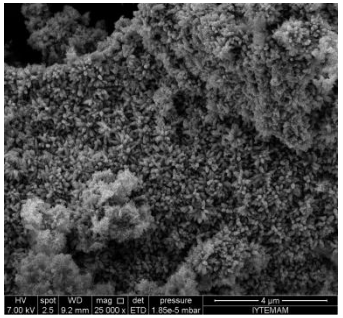
					100 000 X	50 000 X	25 000 X
3	$Zn(NO_3)_2$	-	6	70°C; 2 h	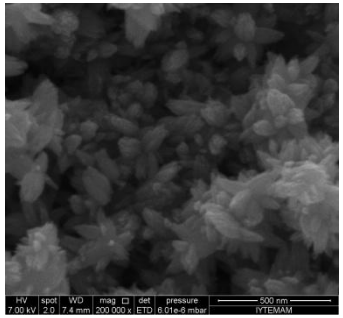	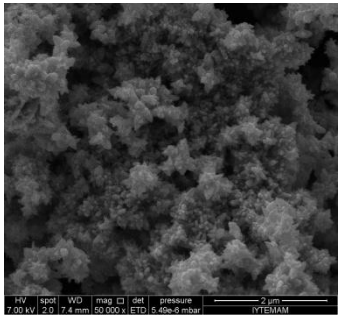	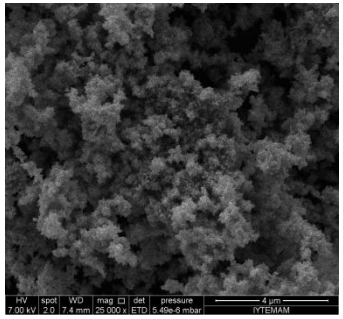
					100 000 X	50 000 X	25 000 X

Table 3.7 (continued) SEM images of Experiments 2 to 8

Exp. No	**Zn^{2+} salt**	**Additive**	**$\frac{[OH^-]}{[Zn^{2+}]}$**	**Reaction Conditions**	**Scale of SEM Images**		
4	$Zn(NO_3)_2$	-	3	20°C; 30 min. 90°C; 6 h	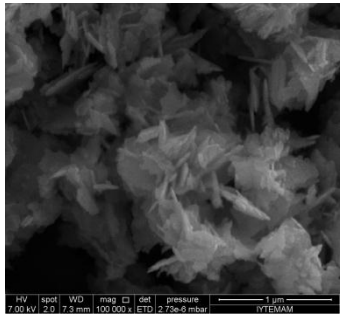	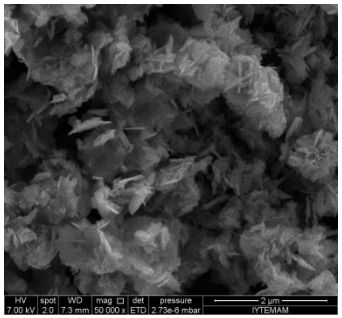	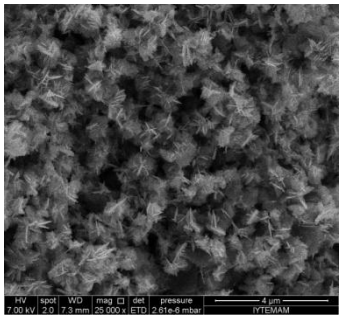
					100 000 X	50 000 X	25 000 X
5	$ZnSO_4$	NH_3	4	5°C; 1 h 20°C; 1.5 h 90°C; 5 h	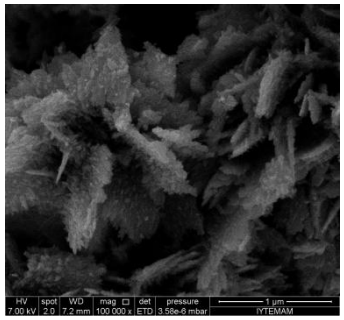	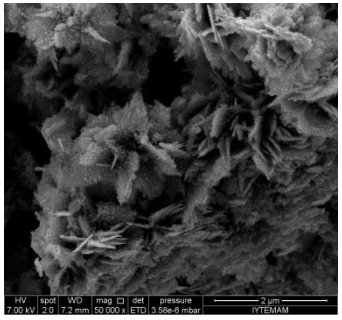	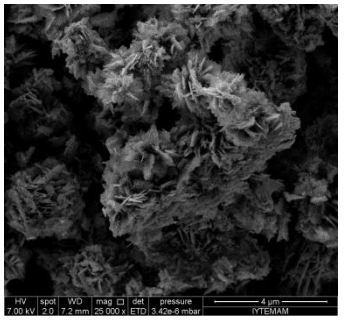
					100 000 X	50 000 X	25 000 X

Table 3.7 (continued) SEM images of Experiments 2 to 8

Exp. No	**Zn^{2+} salt**	**Additive**	**$\frac{[OH^-]}{[Zn^{2+}]}$**	**Reaction Conditions**	**Scale of SEM Images**		
6	$ZnSO_4$	SDS	4	5^oC; 1 h 20^oC; 1.5 h 90^oC; 5 h	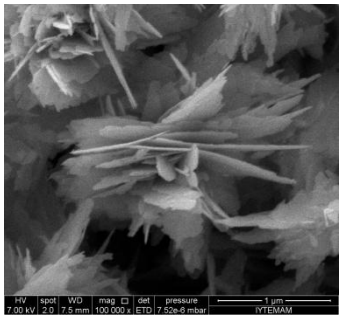	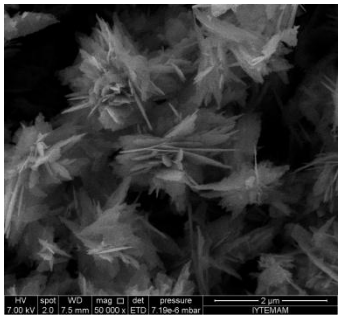	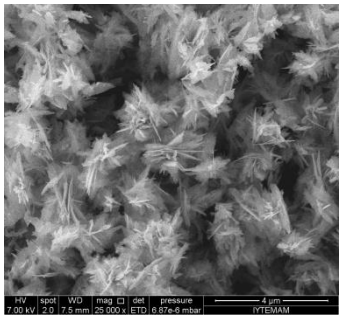
					100 000 X	50 000 X	25 000 X
7	$ZnCl_2$	SDS	6	5^oC; 3 min. 20^oC; 2 h 85^oC; 5 h	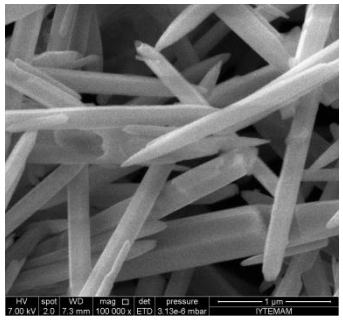	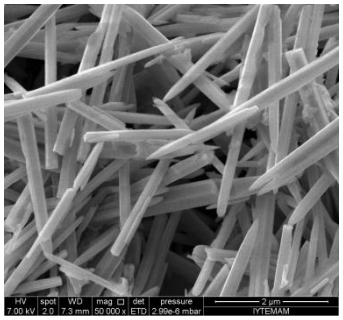	
					100 000 X	50 000 X	25 000 X

Table 3.7 (continued) SEM images of Experiments 2 to 8

Exp. No	Zn^{2+} salt	Additive	$\frac{[OH^-]}{[Zn^{2+}]}$	Reaction Conditions	Scale of SEM Images		
8	$ZnCl_2$	SDS	6	5°C; 3 min. 85°C; 5 h	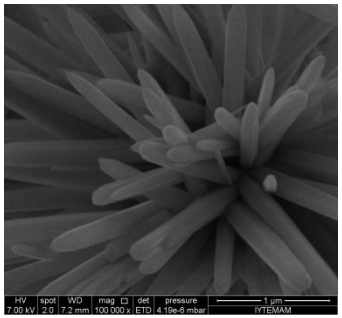	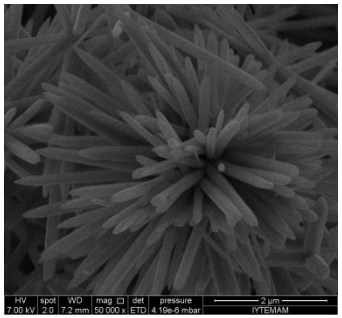	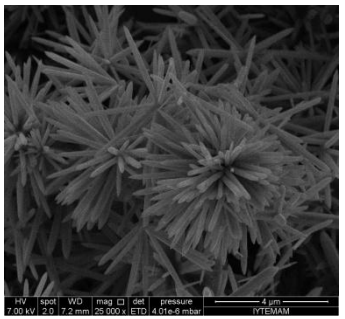
					100 000 X	50 000 X	25 000 X

The summary of Experiments 2 to 8 are given in Table 3.8.

Table 3.8 The summary of Experiments 2 to 8 in terms of morphology obtained under the given experimental conditions

Exp. No	**Zn^{2+} salt**	**Add.**	$\frac{[OH^-]}{[Zn^{2+}]}$	**Reaction Conditions**	**Morphology of Synthesized ZnO**
2	$Zn(NO_3)_2$	-	2	70^{o}C; 2 h	Flowers formed by short rods
3	$Zn(NO_3)_2$	-	6	70^{o}C; 2 h	Flowers
4	$Zn(NO_3)_2$	-	3	20^{o}C; 30 min. 90^{o}C; 6 h	Connected plates
5	$ZnSO_4$	NH_3	4	5^{o}C; 1 h 20^{o}C; 1.5 h 90^{o}C; 5 h	Connected plates
6	$ZnSO_4$	SDS	4	5^{o}C; 1 h 20^{o}C; 1.5 h 90^{o}C; 5 h	Plates with serrated edges
7	$ZnCl_2$	SDS	6	5^{o}C; 15 min 20^{o}C; 2 h 85^{o}C; 5 h	Rods
8	$ZnCl_2$	SDS	6	5^{o}C; 15 min 20^{o}C; 2 h 85^{o}C; 5 h	Connected rods

3.2.2 XRD analysis

The crystal structure of the nanoparticles are identified using Phillips X'Pert Pro X-ray diffraction (XRD) with CuKα radiation (λ=1.5418Å) in a 2 θ range of 10-90°.

XRD results show that, all nanoparticles produced under different reaction conditions have wurtzite hexagonal crystal structure (JCPDS Card no: 36-1451).

In hexagonal geometry the lateral planes of the crystal are oriented in six non-orthogonal directions in addition there are also top and bottom places of the

hexagonal geometry. Therefore, fractional numbers have to be used in showing the directions of the hexagonal plane in terms of rectangular coordinates.

For planes, the index is thereciprocal of the value of the intersection of the plane with aparticular axis, converted to whole numbers. For directions, the index is the axis coordinate of the end point of the vector, converted to nearest whole numbers given in Table 3.9.

Table 3.9 Growth directions for XRD peaks

	(100)	(002)	(101)	(102)	(110)	(103)	(200)	(112)	(201)
x	1	0	1	1	1	1	1/2	1	1/2
y	0	0	0	0	1	0	0	1	0
z	0	1/2	1	½	0	1/3	0	1/2	1

The XRD results of Experiments 2 to 8 are given in Figure 3.1 (a-g). That the highest intensity peak belongs to the (101) crystal plane indicates growth in both diameter and length of particles.

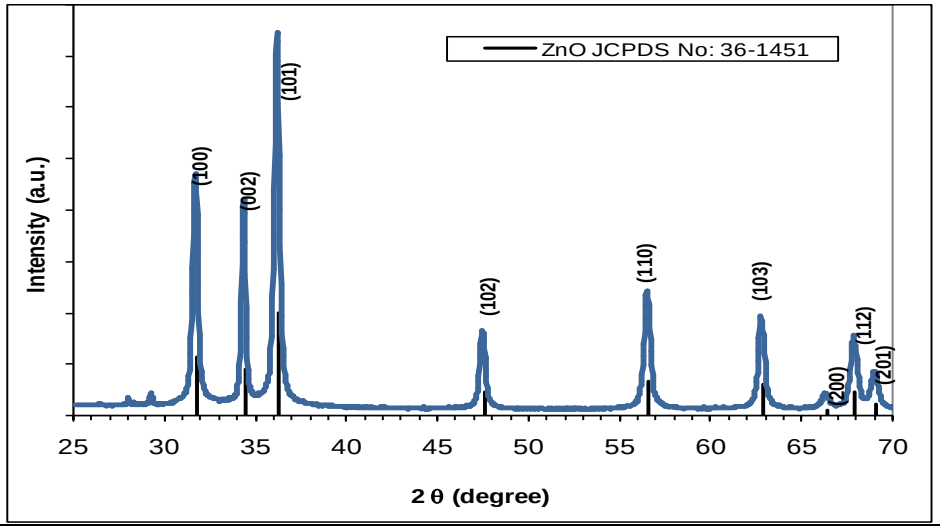

a) Experiment 2: Flowers formed by short rods

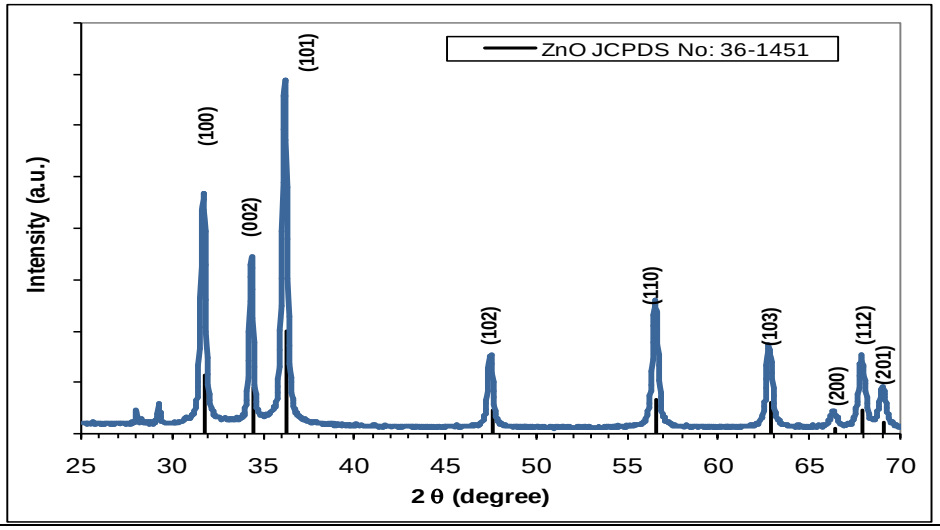

b) Experiment 3: Flowers

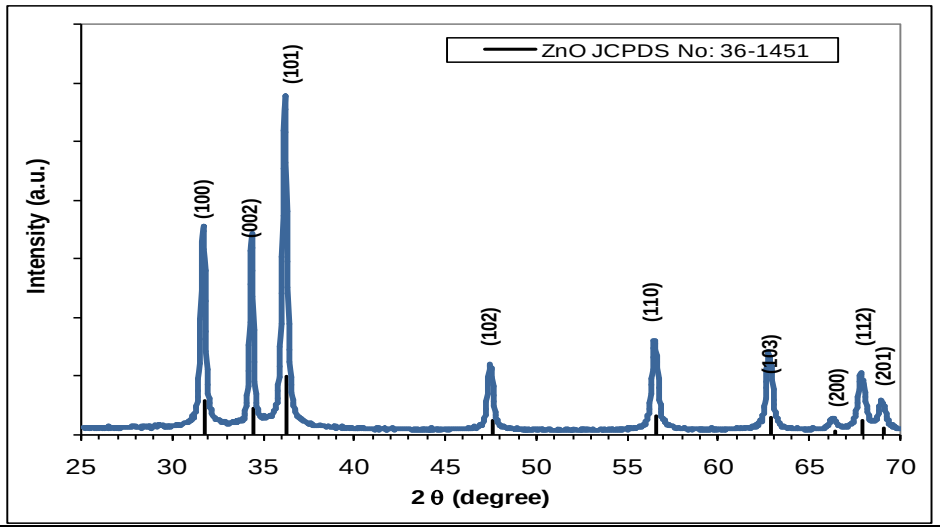

c) Experiment 4: Connected plates

Figure 3.1 Peaks obtained in XRD for Experiments 2 to 8

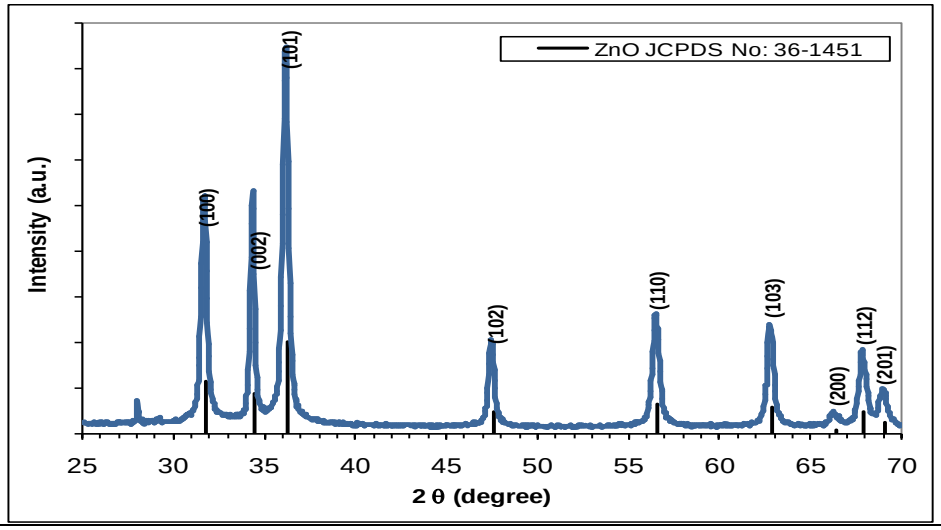

d) Experiment 5: Connected plates

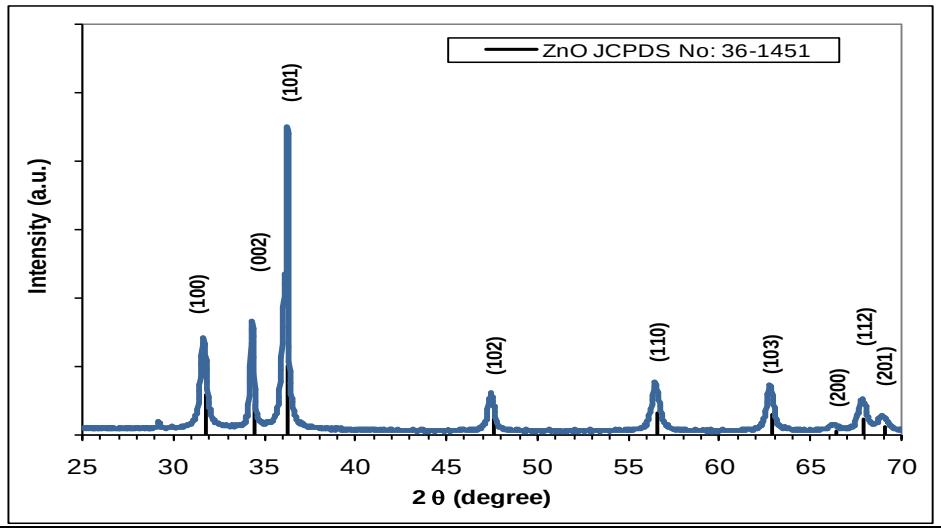

e) Experiment 6: Plates with serrated edges

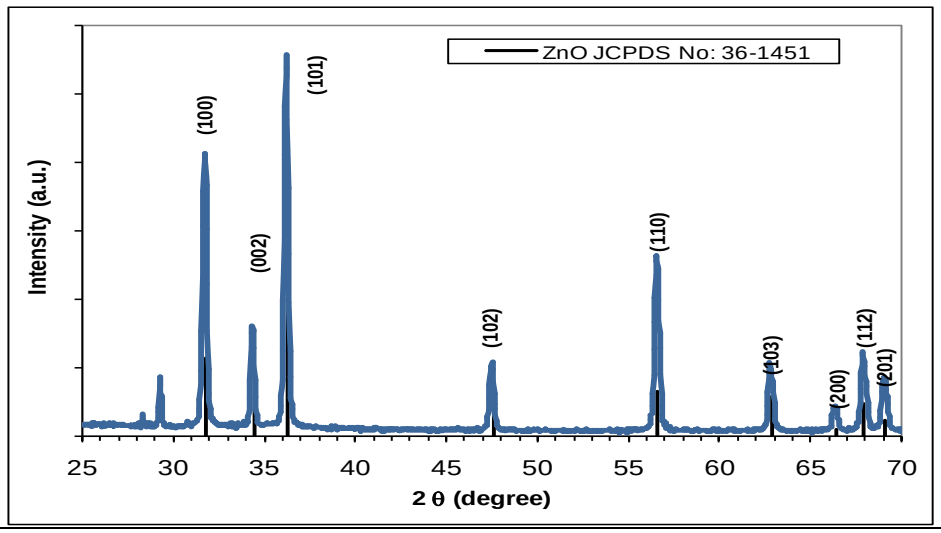

f) Experiment 7: Rods

Figure 3.1 (continued) Peaks obtained in XRD for Experiments 2 to 8

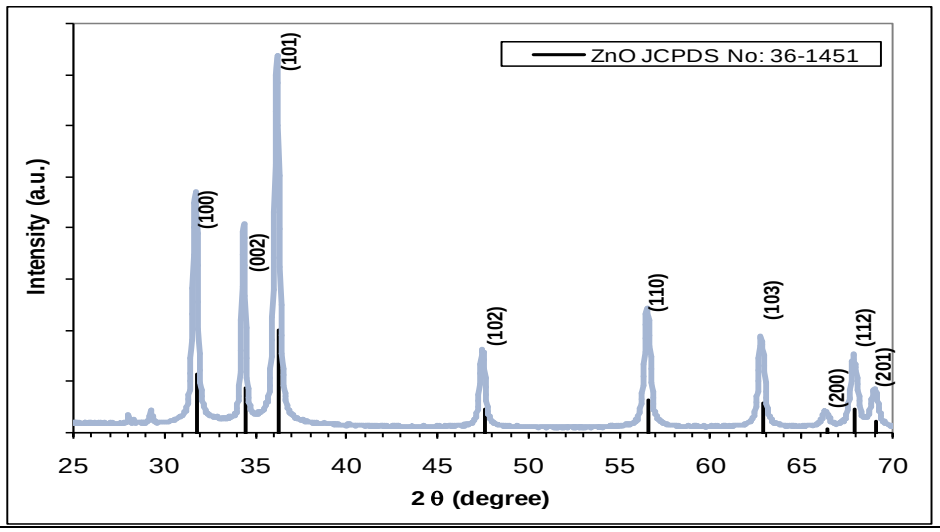

g) Experiment 8: Connected Rods

Figure 3.1 (continued) Peaks obtained in XRD for Experiments 2 to 8

A typical sheet like structure is observed in Experiment 6 given in Figure 3.1. The corresponding XRD peak given in the same figure has the maximum peak in (101) direction. The peak corresponding to this direction is the maximum in all cases. Therefore it does not indicate the morphology by itself. The relative highest of the other peaks are important, as well. In the case of plane sheets is in the case of experiments 6 both (100) and (002) peaks are low as well as the peaks corresponding to higher diffraction angles.

On the other hand, the other extreme of rod shaped particles are obtained in Experiment 7 and 8. The relative height of (100) and (101) peaks indicate the length of the rods. If the rods are long then (101) is near the same height as (100) in the case of Experiment 7. If the rods are short and bundled together than there is a large difference between (100) and (101) peaks; in addition, (002) peak also increases.

Crystallite size is determined by using Scherrer's equation in XRD. D_{grain} of synthesized ZnO nanoparticles is calculated from XRD peaks. The calculations are given in Appendix B.

Results obtained from Scherrer's equation for (101) plane is given in Table 3.10.

Table 3.10 Grain size of synthesized ZnO nanoparticles

Exp No	**Morphology of Nanoparticles**	**2θ (degree) for 101 peak**	**Intensity of (101)**	**FWHM (degree)**	**D_{grain} (nm)**
2	Flowers	36.15	3750	0.33	25.84
3	Flowers	36.15	3450	0.32	26.68
4	Connected Plates	36.15	5800	0.30	28,54
5	Connected Plates	36.14	4250	0.35	24.31
6	Plates with serrated edges	36.15	4600	0.30	28.54
7	Rods	36.18	2560	0.25	34.62
8	Connected rods	36.15	3800	0.31	27.58

The larger grain size and smaller full width at half maximum (FWHM) values indicate better crystallization of nanoparticles. The results show that highest crystalinity of the nanoparticles is obtained in Experiment 7. This is due to the continuity of the shape of the rods. The other shapes have smaller size planes connected together. Therefore, their grain size is low and direction of crystallinty, intermittent.

3.2.3 Optical characterization

The diffuse reflectance spectra of nanoparticles are measured using Shimadzu UV-2600-ISR UV/Vis spectrophotometer with integrating sphere attachment (λ=200-800nm).

Reflectance value shows the behaviour of ZnO powders under UV lights given in Figure 3.2.

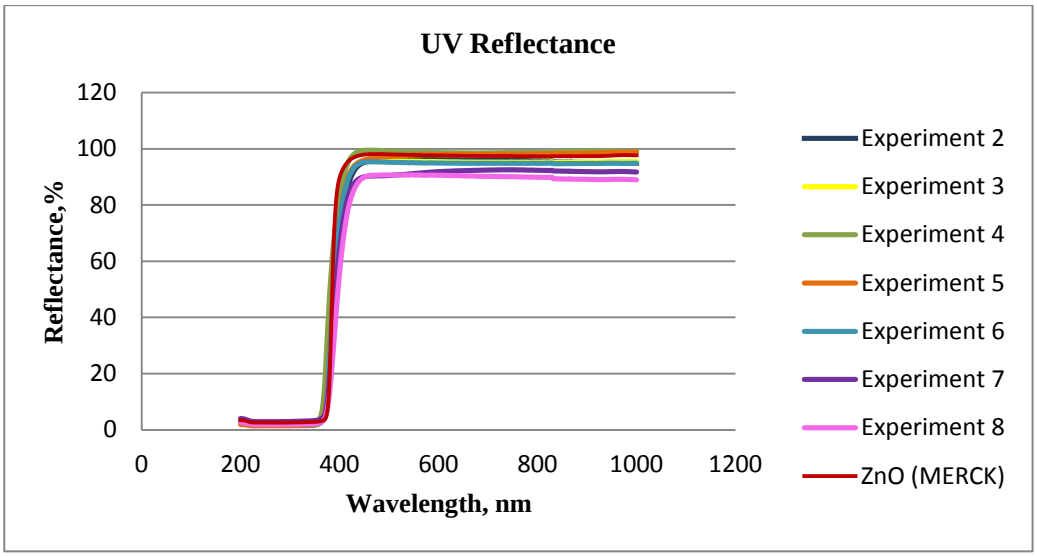

Figure 3. 2 Reflectance of ZnO powders

Reflectance value shows the behaviour of ZnO powders under UV lights. UV lamps emit ultraviolet energy at 315 – 400 nm. If ZnO powders reflect UV lights at 315– 400 nm, the UV lights can not be absorbed by varnish. As a result of this, the degradation can not be occured in varnish film. Depending on this, color change is not observed.

The differences of reflectance values between ZnO powders are shown in Figure 3.3.

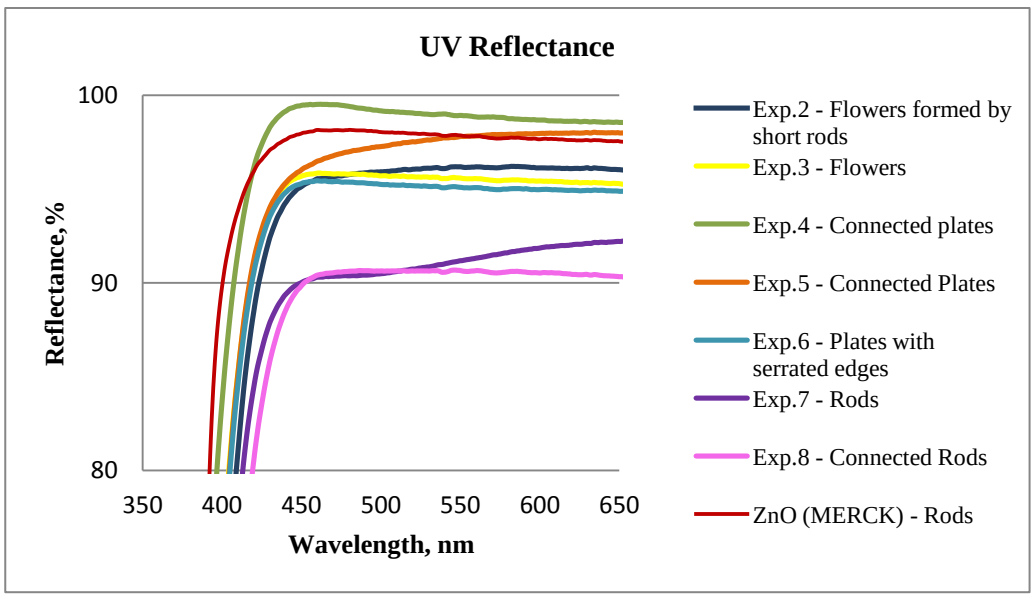

Figure 3. 3 The differences of reflectance values between ZnO powders

The effect of morphology on reflectance values are shown clearly in Figure 3.3. However, the highest point of reflectance and reaching this point at which wavelength are determined showed in Figure 3.4. According to Figure 3.4, the values of **λ,** R_{act} and R_{cur} are summarized in Table 3.11.

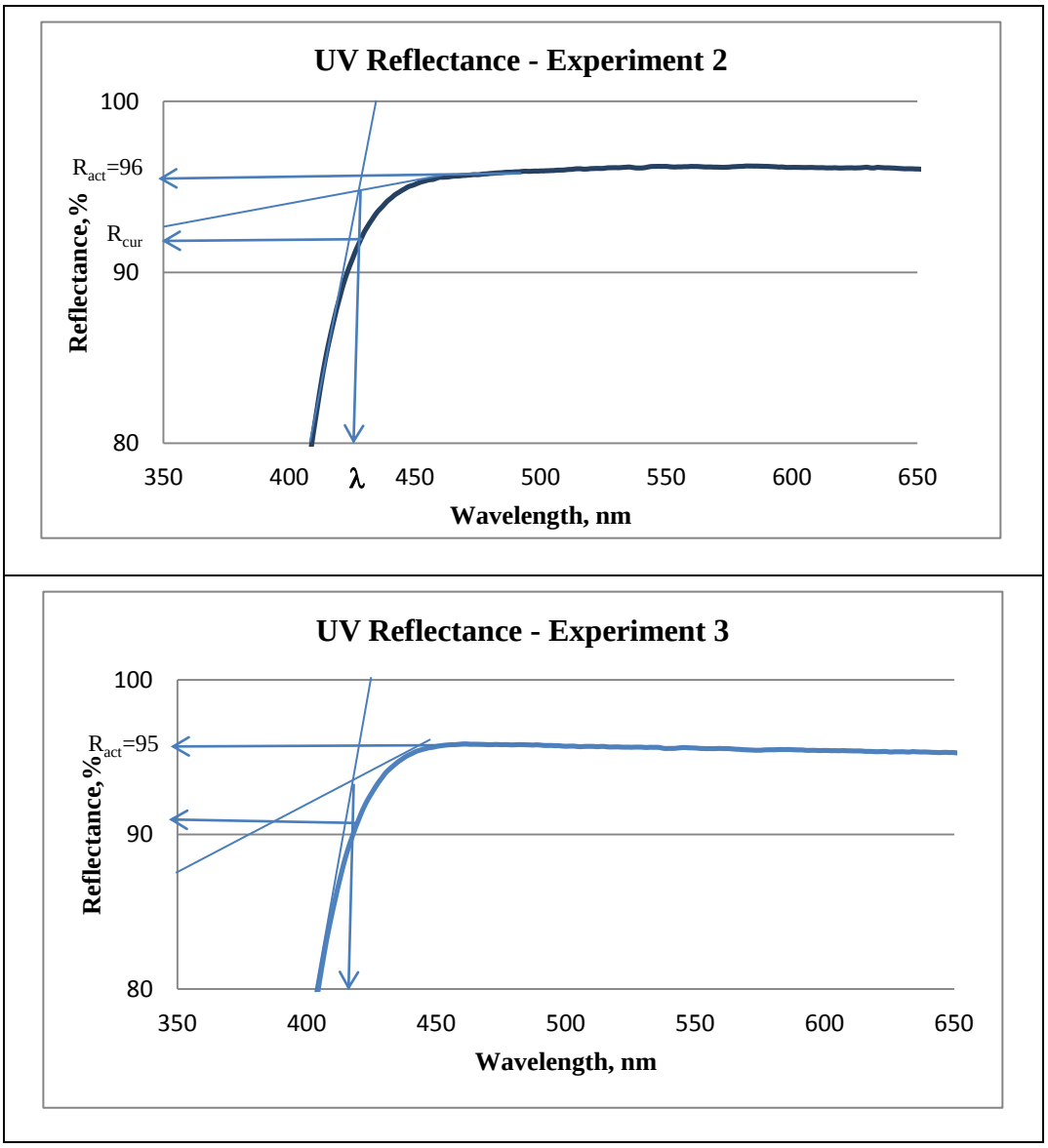

Figure 3.4 Determination of **λ,** R_{act} and R_{cur}

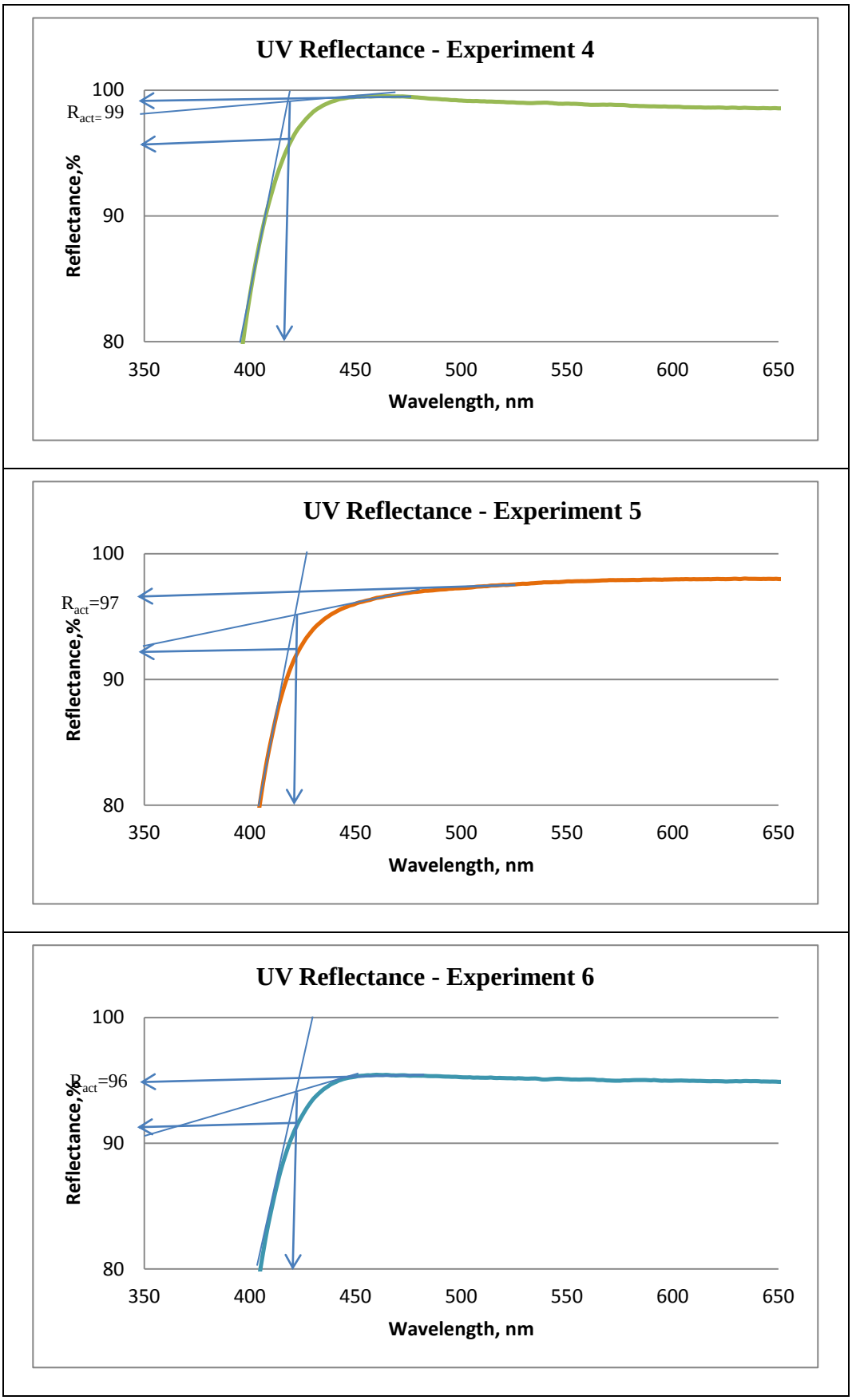

Figure 3.4 (continued) Determination of **λ,** R_{act} and R_{cur}

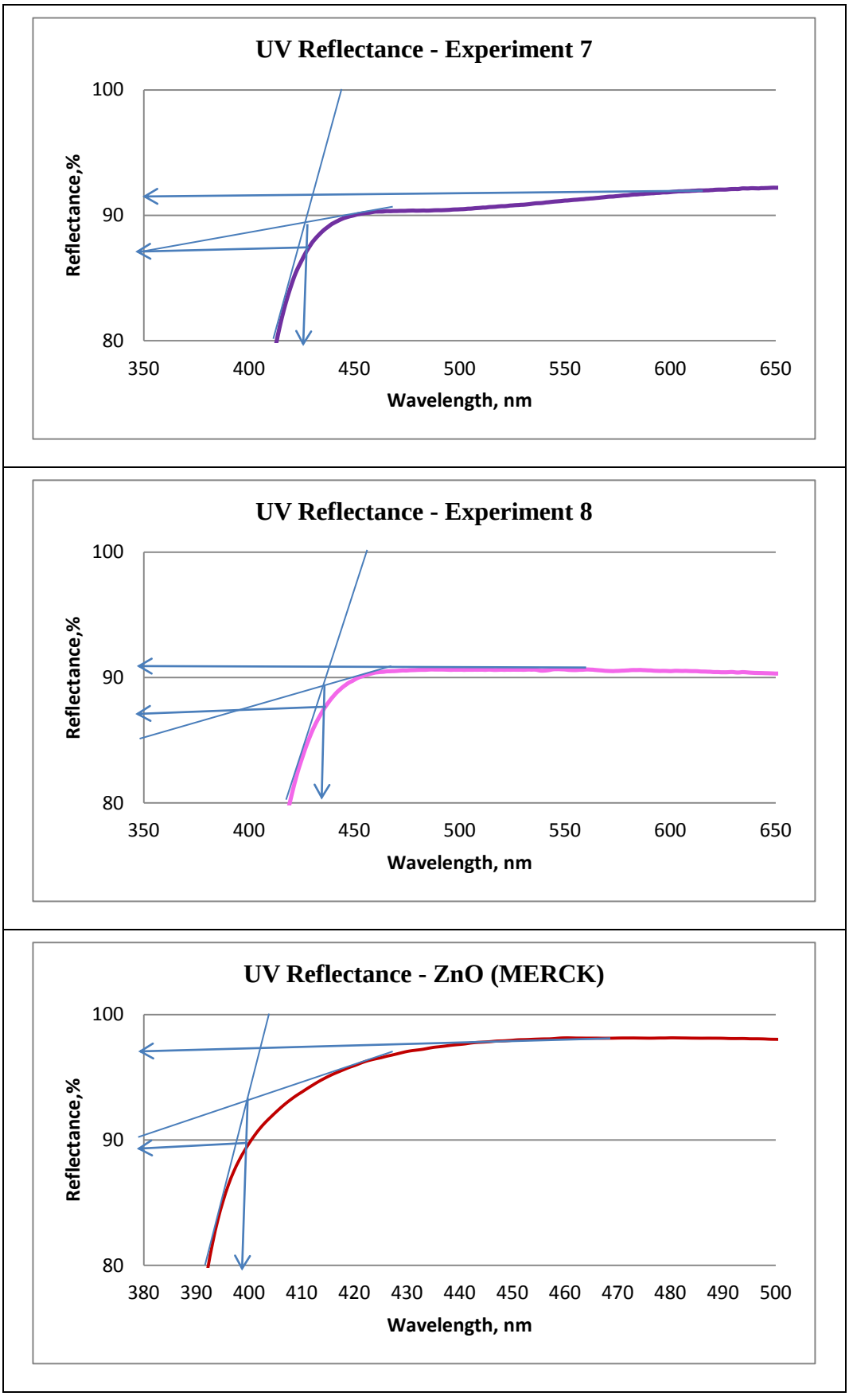

Figure 3.4 (continued) Determination of **λ,** R_{act} and R_{cur}

R_{cur} of Experiment 4 is the highest value, R_{cur} of Experiment 7 and 8 are the lowest value among the experiments. It is related with their morphologies. Rods and connected rods are formed with Experiment 7 and 8, respectively. Connected plates are formed with Experiment 4. According to values of reflectance, R_{cur} is increased with increasing surface area. Connected sheets have much more surface area than rods.

In fact that, as all the nano particles have the same composition, they reflect totally the UV-light. The differences between the morphologies have subtle effects: The sharpness of the transition and the total reflection in the visible region. This intern depend on have closely the nano particles can be packed together and total surface area.

Indicates, ΔR how steep the curve is that is the wavelength interval, $\Delta\lambda$ over which the nano particles change overfrom total reflectanceto total absorbance.

This is found to be a functional the voidage between the nano particles. The less the voidage, the steeper is the curve and the more sharp is the transition. The more the voidage, the less is the final absorbance and more gradual is the transition.

If ZnO powders reflect UV lights at 315– 400 nm, the UV lights can not be absorbed by varnish.

Table 3.11 The values of **λ,** R_{act} and R_{cur} of ZnO synthesized with Experiments 2 - 8

Exp.No	**Morphology**	**λ**	**R_{actual}**	**R_{cur}**
2	Flowers formed by short rods	428	95.8	92
3	Flowers	421	96	92
4	Connected Plates	418	99	95
5	Connected plates	425	97	93
6	Plates with serrated edges	423	95	91.8
7	Rods	428	90.2	87.8
8	Connected rods	438	90.8	88
MERCK	Rods	402	98	91.8

λ value is at which ZnO nanoparticles reflect UV lights. Reflection value indicates that the percentage of UV lights reflected by ZnO nanoparticles at λ value. The smaller λ value and higher reflectance value indicate better UV reflection performance. Experiment 4 has the highest reflectance value at lowest λ value.

Minumum energy requirement for the photoactivity of ZnO particles (Eg) in UVA range is calculated from Reflectance measurements using Kubelka-Munk function given in Appendix C. Below the critical λ values given in Table 3.12, 100% of UVA light is absorbed.

Table 3.12 Band Gap Energy (Eg) of ZnO nanoparticles

Exp. No	**Morphology**	**$\lambda_{critical}$ (nm)**	**Band Gap Energy (Eg) , eV**
2	Flowers formed by short rods	375	3.31
3	Flowers	371	3.34
4	Connected plates	367	3.38
5	Connected plates	373	3.32
6	Plates with serrated edges	375	3.31
7	Rods	377	3.29
8	Connected rods	377	3.29
MERCK	Rods	378	3.38

Band gaps of the different morphologies vary between 367-378 nm Experiment 4 reflects the UV lights at shorter wavelength – 367 nm. It means that the UV reflection begins earlier compared to other experiments.

3.3 The Change in ZnO Nanoparticles After Dispersion in Solvent of Varnish

ZnO powders synthesized by Experiments 2 to 8 are dispersed in butyl acetate to observe the change in the morphology (tendency of the ZnO nanoparticles to break under the imposed shear) during the dispersion process. The dispersion time is 30 minutes and the impeller speed is 2000 rpm. The SEM

results of ZnO powders dispersed in butyl acetate are given in Table 3.13. The variation in the structures is not appreciable. One reason could be the low viscosity and hence the low impact of the solvent on the nanoparticles.

The dispersion of ZnO nano particles in acrylic varnish is very important for efficient UV stabilization. The desired condition is the homogenous dispersion of ZnO powders in acrylic varnish. Yet, the morphology of ZnO particles should not be changed under the dispersion conditions.

The ZnO powders retain their morphologies and homogeneity of the dispersion as can be observed in Table 3.13: No appreciable agglomeration has taken place as indicated in the SEM results. The comparison between ZnO powders after production and ZnO powders after dispersion in butyl acetate is given in Table 3.14.

Table 3.13 The SEM images of ZnO powders dispersed in butyl acetate

Exp. No	2	3	4
Scale: 100 000 X	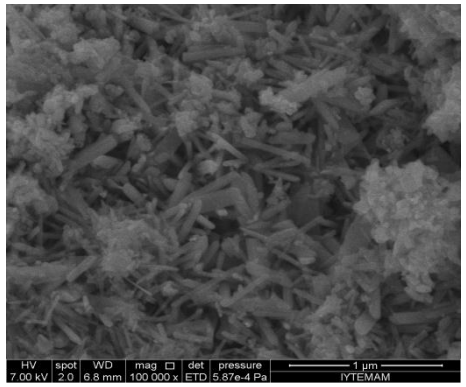	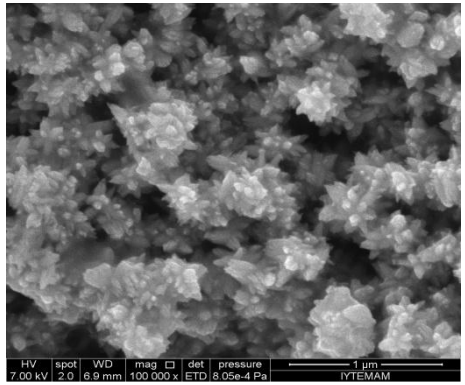	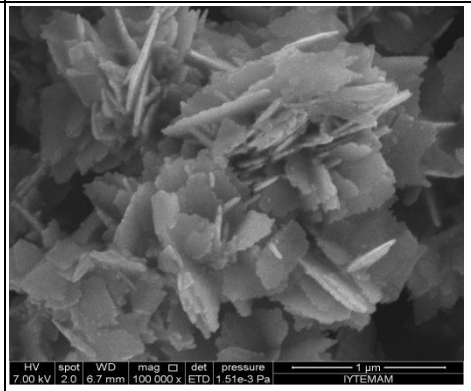
Scale: 20 000 X	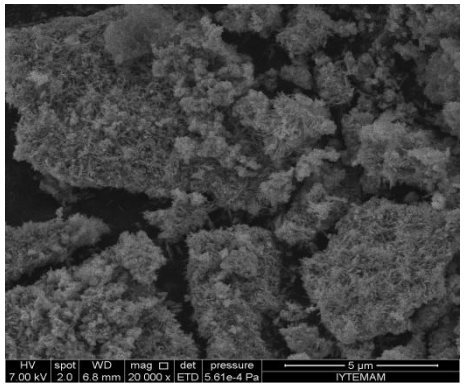	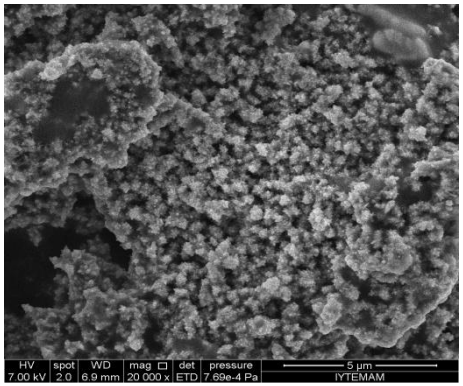	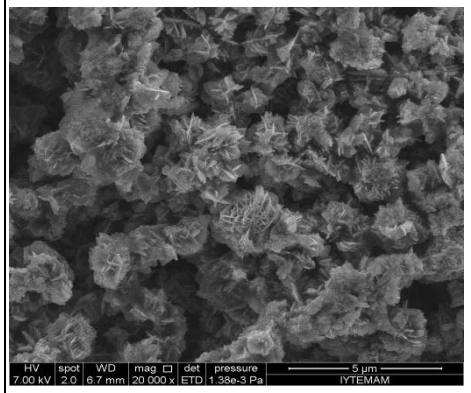

Table 3.13 (continued) The SEM images of ZnO powders dispersed in butyl acetate

Exp. No	5	6	7
Scale: 100 000 X	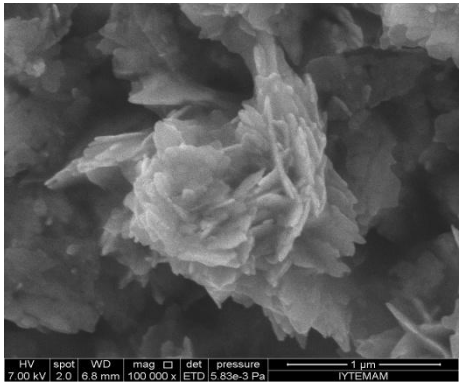	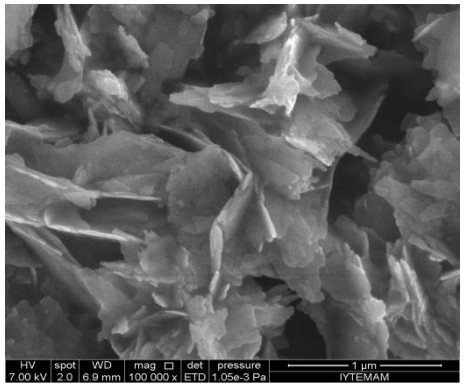	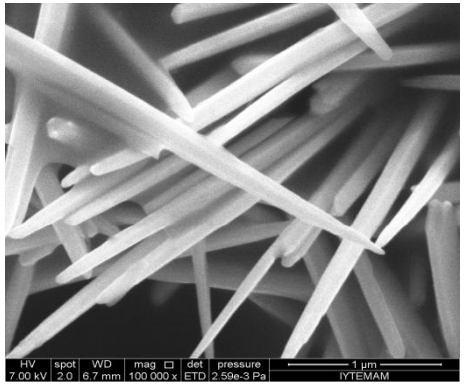
Scale: 20 000 X	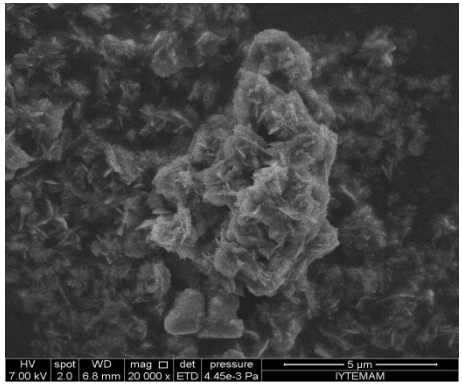	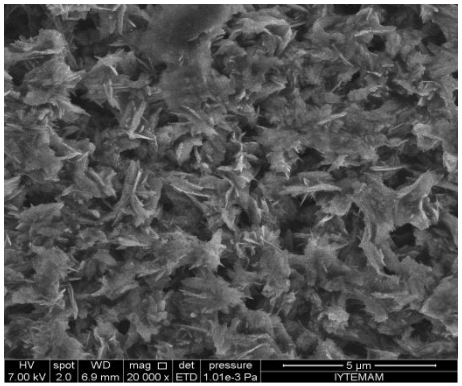	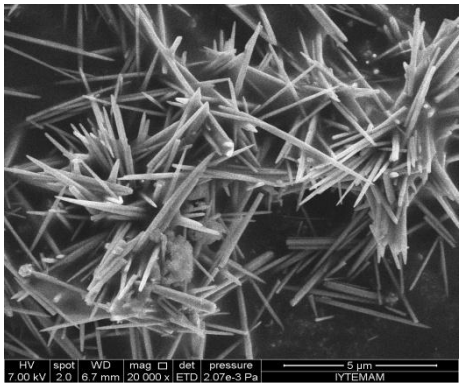

Table 3.14 The comparison between ZnO powders after production and ZnO powders after dispersion in butyl acetate

Exp.No	After Production		After Dispersing in Butyl Acetate	
	Unit Morphology	**SEM Results**	**Unit Morphology**	**SEM Results**
2	Flowers formed by short rods	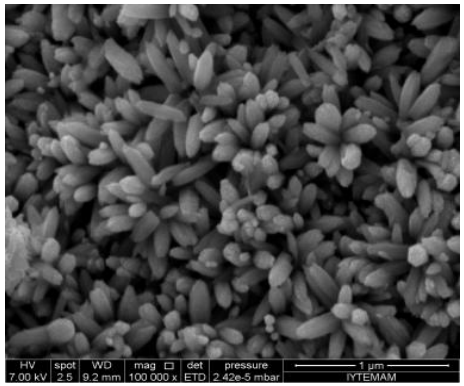	Mixed Typed (flowers and rods)	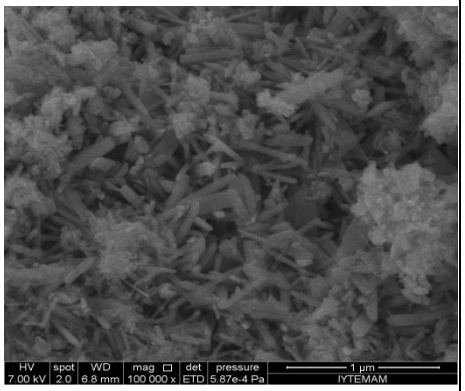
3	Flowers	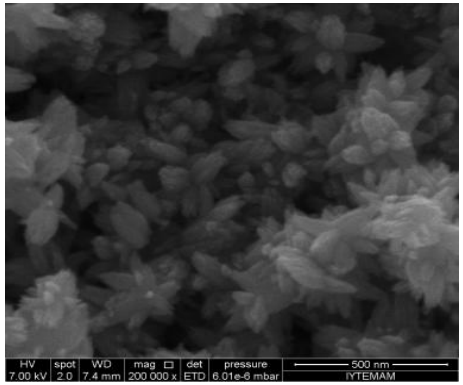	Flowers	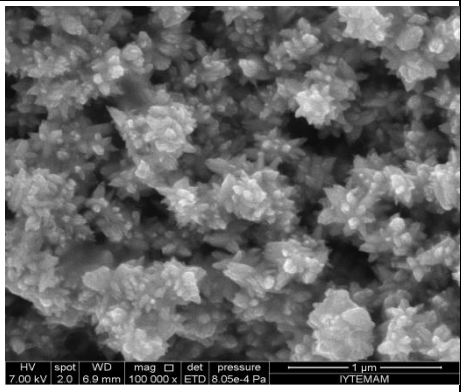

Table 3. 14 (continued) The comparison between ZnO powders after production and ZnO powders after dispersion in butyl acetate

Exp.No	After Production		After Dispersing in Butyl Acetate	
	Unit Morphology	**SEM Results**	**Unit Morphology**	**SEM Results**
4	Connected Plates	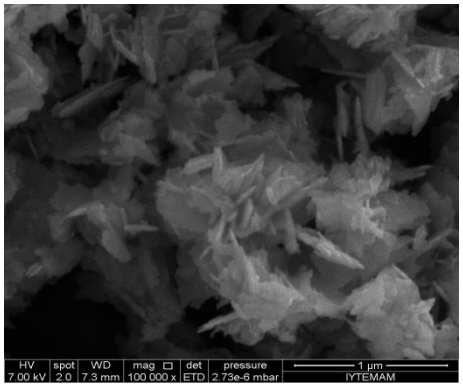	Connected plates	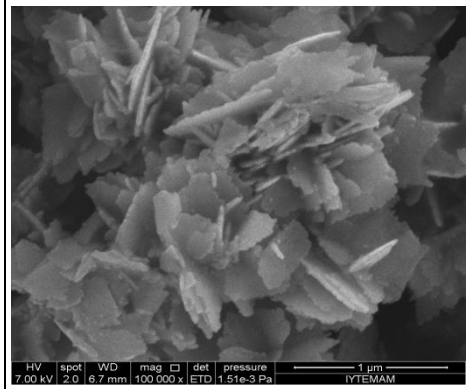
5	Connected Plates	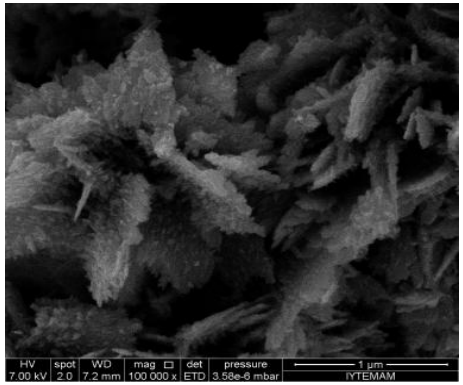	Connected plates	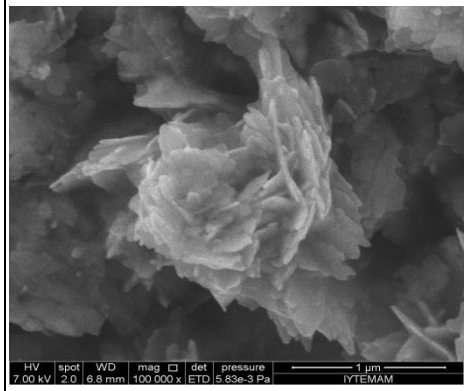

Table 3.14 (continued) The comparison between ZnO powders after production and ZnO powders after dispersion in butyl acetate

Exp.No	After Production		After Dispersing in Butyl Acetate	
	Unit Morphology	**SEM Results**	**Unit Morphology**	**SEM Results**
6	Plates with serrated edges	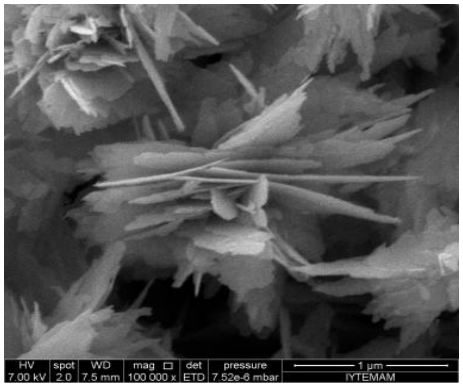	Plates with serrated edges	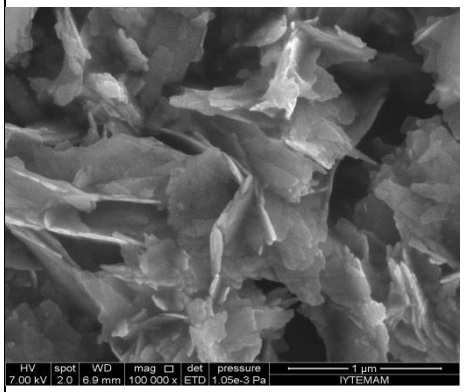
7	Rods	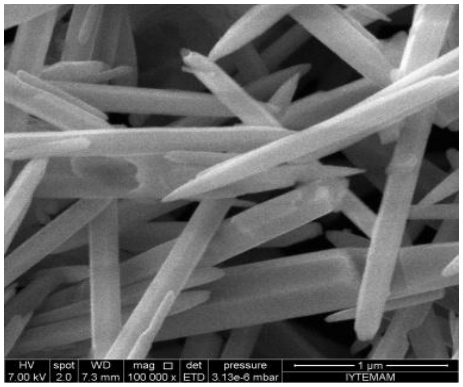	Rods	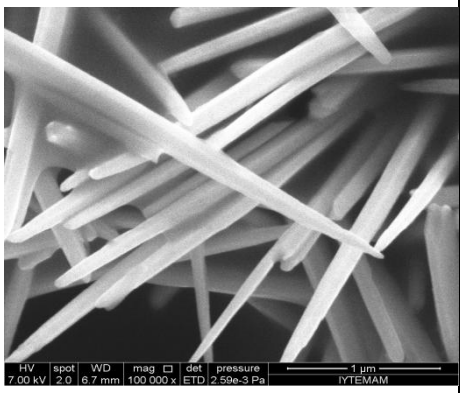

Table 3. 14 (continued) The comparison between ZnO powders after production and ZnO powders after dispersion in butyl acetate

Exp.No	After Production		After Dispersing in Butyl Acetate	
	Unit Morphology	**SEM Results**	**Unit Morphology**	**SEM Results**
8	Connected rods	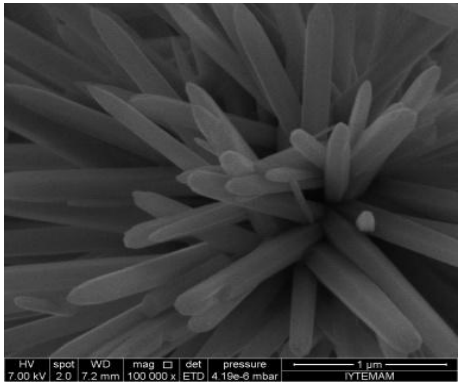	Connected rods	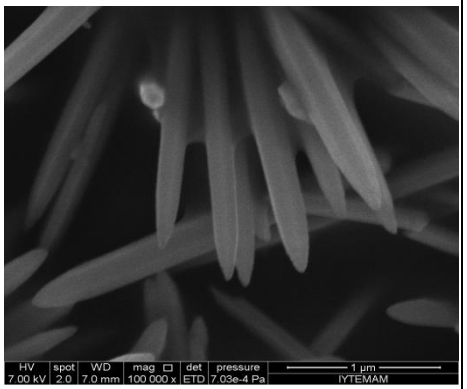

3.4 UV Stabilizing Test

ZnO powders synthesized are dispersed in acrylic varnish. Varnish is applied on a glass for UV stabilizing test. After UV stabilizing test, the color changes are determined. Color change gives how varnish is resistant against UV lights. X-rite spectrophotometry is used to determine color change. Δ represents the difference between standart and sample. The standart does not include ZnO nanoparticles. So, if standard exposed to UV radiation is compared with sample exposed to UV radiation, the UV stabilizing effect of ZnO can be observed.

After UV test, the color changes are obtained by X-rite spectrophotometer. First, color of the part of varnish that is not expose the UV lights are determined. That is the reference part. Then, color of the part of varnish that is exposed to UV lights are determined. The color differences of these parts gives how color of varnish is changed under UV lights. delB is the the color change of acrylic varnish under UV lights. The acceptable value of delB is smaller than 0.5. delB values are given in Table 3.15.

delB values are smaller than 0.5 for the experiments. It means that, addition of ZnO powders synthesized with experiments provide UV resistance for acrylic varnish.

However, morphological effect on UV test can be seen clearly. ZnO powders synthesized with Experiment 4, 5 and 6 give the most effective UV stability results. The morphologies of Experiment 4 and 5 is connected plates. Experiment 6 has plates with serrated edges morphology. Among the experiments, Experiment 6 has the lowest delB value. Because of its serrated edges, the surface area is more than others.

Experiment 8 has the greater delB value among the experiments. Nevermore, delB is smaller than 0.5 that is acceptable value. The reason of the greater delB is 3D connected rods morphology. Also, the reflectance values are related with delB values given in Table 3.15.

Table 3.15 UV test results of Experiments 2 to 8

Morphology	**Sem Result**	**delb**	**λ**	**R_{cur}**	**R_{actual}**
Flowers formed by short rods	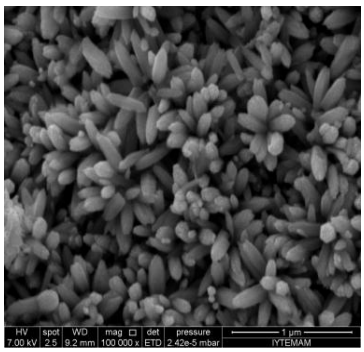	0.25	420	92	96
Flowers	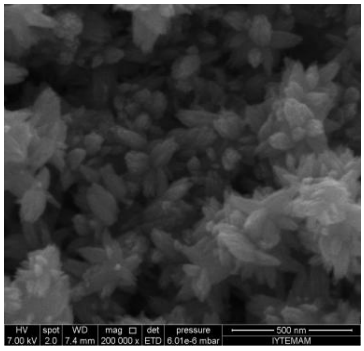	0.30	410	91	95
Connected Plates	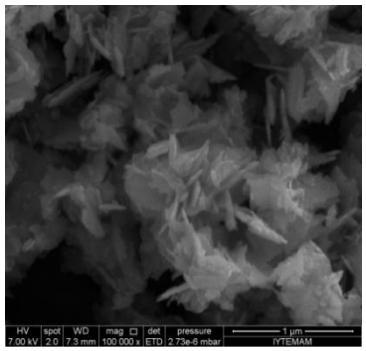	0.10	430	96	99
Connected plates	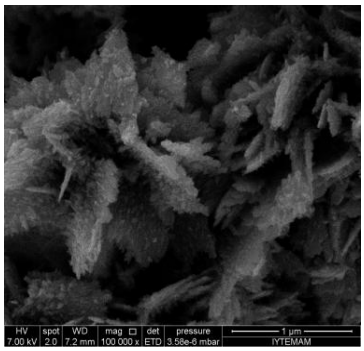	0.07	410	93	97

Table 3.15 (continued) UV test results of Experiment 2 to 8

Morphology	**Sem Result**	**delb**	**λ**	**R_{cur}**	**R_{actual}**
Plates with serrated edges	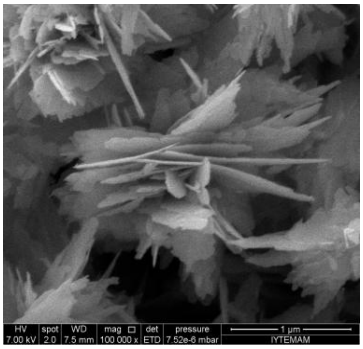	0.05	410	91	95
Rods	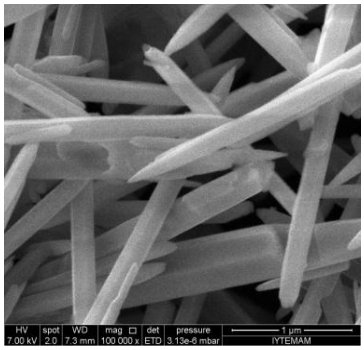	0.30	410	87	91
Connected Rods	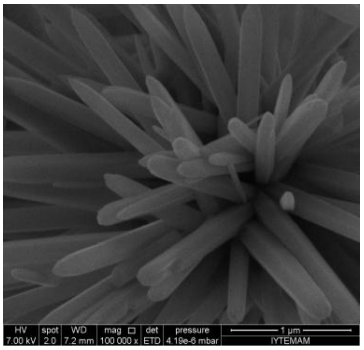	0.35	410	87	91

The R_{cur} of Experiment 7 and 8 is the lowest value amoung the experiments. However, the delB values are the highest than others. The morphology is formed by rods. Experiment 4, 5 and 6 have the smallest delB value. Connected sheets formed provide the best UV resistance. Additionally, the reflectance values are highest than others.

Experiment 2 and 3 have the same behaviour with Experiment 7 and 8.

According to these results, it can be said that the efficiency of ZnO powders are related with reflectance value and also its morphology.

Rods and flowers liked morphologies have the lowest UV stability. However, connected plates morphologies have the most efficient for UV stability.

5.0 CONCLUSION

The performance of wood can be significantly enhanced by incorporation of nanoparticles in the coatings. Wood polymers are degraded due to UV light irradiation which resulted in color changes on wood surfaces. UV absorbers are used in wood coating to prevent against UV radiation.

The aim of this study is that investigate the morphological effect of zinc oxide nanoparticles on UV stabilization for wood coatings. Hydrothermal method is used to synthesize zinc oxide nanoparticles. Different morphologies are obtained suc as flower-like, nano sheets, rods by changing the reaction conditions. Their crystal structures, morphologies an optical properties are investigated.

Zinc oxide nanoparticles are dispersed in acrylic varnish and applied on a glass to determine the UV stabilization effect. However, their morphologies, crystal structures and optical properties are associated with UV stabilizing effect.

The best UV stabilization effect is obtained with zinc oxide formed by nano sheets. The yellowish value is 0.07 and the band gap energy is 3.38 eV at 367 nm.

Consequently, according to morphology and surface area, the UV stabilizaiton performance can change. Nano sheets has the best UV stabilizaiton effect due to the highest surface energy.

REFERENCES

Baruwati, B.,Kumar, D., and Manorama, S., 2006, Hydrothermal Synthesis of Highly Crystalline ZnO Nanoparticles: A sensor for LPG and EtOH, Sensors and Actuators, 119, 676-682pp.

Chu, D.,Masuda, Y., Ohji, T., and Kato, K., 2009, Formation and Photocatalytic Applicaiton of ZnO Nanotubes Using Aqueous Solution, Langmuir, 26, 2811-2815pp.

Fan, L. and Song, H., 2006, Hydrothermal Synthesis and Photoluminescent Properties of ZnO Sub-Micrometer and Micrometer Rods, Optical Materials,29, 532-538pp.

Goldschmidt, A., 2007, Basics of Coatings Technology, Vincentz Network, 440-441pp.

Gusatti, M. and Barrosso, G., 2008, Synthesis of ZnO Nanostructures in Low Reaction Temperature, 476, 88-90pp.

Hajry, A. and Umar, A., 2009, Growth, Properties and Dye-Sensitized Solar Cells- Applications of Zno Nanorods Grown by Low-Temperature Solution Process, Superlattices and Microstructures, 45, 529-534pp.

Jayashree, K.,Pandey, K., and Kavyashree, S., 2012, Polymer Degradation and Stability, 6548.

Li, P.,Liu, H., Xu, F., and Wei, Y., 2008, Controllable growth of ZnO nanowhiskers by a simple solution route, Materials Chemistry and Physics, 112, 393-397pp.

Mahltig, B., Böttcher, H., and Rauch, K., 2005, Optimized UV Protecting Coatings by Combination of Organic and Inorganic UV Absorbers, Thin Solid Films, 485,108-114pp.

Movahedi, M. and Kowsari, E., 2008, A Task Specific Basic Ionic Liquid for Synthesis of Flower Like ZnO by Hydrothermal Method, Materials Letters, 62, 3856-3858pp.

Ni, Y., 2005, Hydrothermal Preparation and Optical Properties of ZnO Nanorods, Materials Science and Engineering, 121, 42-47pp.

Sepeur, S., 2008, Nanotechnology, Vincentz Network, Germany, 69-71pp.

REFERENCES (continued)

Suwanboon, S.,Amornpitoksuk, P., and Muensit, N., 2011, Dependence of Photocataltic Activity on Structural and Optical Properties of Nanocrystalline ZnO Powders,Ceramics International, 37, 2247-2253pp.

Umar, A.,Chauhan, M.S., and Kumar, R., 2011, Large Scale Synthesis of ZnO Balls Made of Fluffy Thin Nanosheets by Simple Solution Process: Structural, Optical and Photocatalytic Properties, Journal of Colloid and Interface Science, 363, 521-528pp.

Usui, H., 2009, The Effect of Surfactants on the Morphology and Optical Properties of Precipitated Wurtzite ZnO, 63, 1489-1499pp.

Wen, S., 2010, Synthesis of ZnO Whiskers via Hydrothermal Decomposition Route, Transections of Nonferrous Metlas Society of China, 20, 1049-1052.

Williams, S., 2009, Finishing of Wood, General Technical Report, 190, 188-190pp.

Xiao, Q., 2008, Synthesis and Characterization of 3D ZnO Nanostructures via A Templete Free Hydrothermal Method, 189, 103-107pp.

Xie, J. and Li, Y., 2009, Simple Fabrication and Photocatalytic Activity of ZnO Particles with Different Morphologies, Powder Technology, 207, 140-144pp.

Xie, J. and Li, P., 2009, Synthesis of Needle and Flower Like ZnO Microstructures by a Simple Aqueous Solution Route, Journal of Physics and Chemistry of Solids, 70, 112-116pp.

Yan, Li. and Feng, H., 2009, Solvo-Thermal Synthesis and Characterization of Nest-Like Zinc Oxide, Transections of Nonferrous Metlas Society of China,20, 119-122pp.

RESUME

Övül KAYAALP is born in Karabük in 1983. She has graduated from high school in 2001. She received her B.S degree in Chemical Engineering Department, Engineering Faculty of Ege University in 2007.

She is working as a Research and Development Engineer at DYO Paint Factory since 2007.

APPENDICES

APPENDIX A

Mole Ratio Calculation of Experiments

Experiment 1:

1 M NaOH; V_{NaOH}: 100mL

$M = \frac{n}{V} 1M = \frac{n}{0.1L} n_{NaOH} = 0.1\text{mol}$

0.5 M $Zn(NO_3)_2.6\ H_2O$; $V_{Zn(NO_3)_2.6\ H_2O}$: 10mL

$M = \frac{n}{V} 0.5M = \frac{n}{0.01L} n_{Zn(NO_3)_2.6\ H_2O} = 0.005\text{mol}$

V_{total}= V_{NaOH} + $V_{Zn(NO_3)_2.6\ H_2O}$ = 100mL + 10mL = 110mL

$V_{precursor\ solution}$ = 30mL

V_{NaOH}= 27.27mL; $V_{Zn(NO_3)_2.6\ H_2O}$ = 2.73mL

1 M NaOH ; V_{NaOH}:27.27mL

$M = \frac{n}{V} 1M = \frac{n}{0.02727L} n_{NaOH} = 0.02727\text{mol}$

0.5M NaOH ; $V_{Zn(NO_3)_2.6\ H_2O}$: 2.73mL

$M = \frac{n}{V} 0.5M = \frac{n}{0.00273L} n_{Zn(NO_3)_2.6\ H_2O} = 0.00137\text{mol}$

$$\frac{n_{NaOH}}{n_{Zn(NO_3)_2.6\ H_2O}} = \frac{0.02727\ mol}{0.00137\ mol} = 20$$

Experiment 2:

1M NaOH ; V_{NaOH}: 100mL

$M = \frac{n}{V} 1M = \frac{n}{0.100\ L} n_{NaOH} = 0.1\text{mol}$

0.5M $Zn(NO_3)_2.6\ H_2O$; $V_{Zn(NO_3)_2.6\ H_2O}$: 100mL

$M = \frac{n}{V} 0.5M = \frac{n}{0.100\ L} n_{Zn(NO_3)_2.6\ H_2O} = 0.05\text{mol}$

$V_{total}=V_{NaOH} + V_{Zn(NO_3)_2.6\ H_2O}$ = 100mL + 100mL = 200 mL

$[OH^-]= \frac{0.1mol}{0.200L} [OH^-] = 0.5\text{M}$

$[Zn^{2+}]= \frac{0.05mol}{0.200L} [Zn^{2+}] = 0.25\text{M}$

$$\frac{[OH^-]}{[Zn^{2+}]} = \frac{0.5M}{0.25M} = 2$$

Experiment 3:

1M NaOH ; V_{NaOH}: 120mL

$M = \frac{n}{V} 1M = \frac{n}{0.120\ L} n_{□aOH} = 0.12\text{mol}$

0.5M $Zn(NO_3)_2.6\ H_2O$; $V_{Zn(NO_3)_2.6\ H_2O}$: 40mL

$M = \frac{n}{V} 0.5M = \frac{n}{0.04\ L} n_{Zn(NO_3)_2.6\ H_2O} = 0.02\text{mol}$

$V_{total}=V_{NaOH} + V_{Zn(NO_3)_2.6\ H_2O}$ = 120mL + 40mL = 160 mL

$[OH^-]= \frac{0.12mol}{0.160L} [OH^-] = 0.75\text{M}$

$[Zn^{2+}]= \frac{0.02mol}{0.160L} [Zn^{2+}] = 0.125\text{M}$

$$\frac{[OH^-]}{[Zn^{2+}]} = \frac{0.75M}{0.125M} = 6$$

Experiment 4:

1 M NaOH; V_{NaOH}: 120mL

$M = \frac{n}{V} 1M = \frac{n}{0.120L} n_{NaOH} = 0.12\text{mol}$

0.5 M $Zn(NO_3)_2.6\ H_2O$; $V_{Zn(NO_3)_2.6\ H_2O}$: 80mL

$M = \frac{n}{V} 0.5M = \frac{n}{0.08L} n_{Zn(NO_3)_2.6\ H_2O} = 0.04\text{mol}$

$V_{total} = V_{NaOH} + V_{Zn(NO_3)_2.6\ H_2O} = 120\text{mL} + 80\text{mL} = 200\text{mL}$

$[OH^-] = \frac{0.12mol}{0.200L} [OH^-] = 0.6\text{M}$

$[Zn^{2+}] = \frac{0.04mol}{0.200L} [Zn^{2+}] = 0.2\text{M}$

$$\frac{[OH^-]}{[Zn^{2+}]} = \frac{0.6M}{0.2M} = 3$$

Experiment 5:

4M NaOH; V_{NaOH}: 10mL

$M = \frac{n}{V} 4M = \frac{n}{0.010L} n_{NaOH} = 0.04\text{mol}$

0.2M $ZnSO_4.7\ H_2O$; $V_{ZnSO_4.7\ H_2O}$: 50mL

$M = \frac{n}{V} 0.2M = \frac{n}{0.05L} n_{ZnSO_4.7\ H_2O} = 0.01\text{mol}$

$V_{total} = V_{NaOH} + V_{ZnSO_4.7\ H_2O} + V_{additive} = 10\text{mL} + 50\text{mL} + 50\text{mL} = 110\text{mL}$

$[OH^-] = \frac{0.04mol}{0.110L} [OH^-] \cong 0.36\text{M}$

$[Zn^{2+}] = \frac{0.01mol}{0.110L} [Zn^{2+}] \cong 0.09\text{M}$

$$\frac{[OH^-]}{[Zn^{2+}]} = \frac{0.36M}{0.09M} = 4$$

Experiment 6:

4M NaOH; V_{NaOH}: 10mL

$M = \frac{n}{V} 4M = \frac{n}{0.010L} n_{NaOH} = 0.04$mol

0.2M $ZnSO_4.7\ H_2O$; $V_{ZnSO_4.7\ H_2O}$: 50mL

$M = \frac{n}{V} 0.2M = \frac{n}{0.05L} n_{ZnSO_4.7\ H_2O} = 0.01$mol

V_{total}= V_{NaOH} + $V_{ZnSO_4.7\ H_2O}$ + $V_{additive}$= 10mL + 50mL + 50mL = 110mL

$[OH^-]$= $\frac{0.04mol}{0.110L} [OH^-] \cong 0.36$M

$[Zn^{2+}]$= $\frac{0.01mol}{0.110L} [Zn^{2+}] \cong 0.09$M

$$\frac{[OH^-]}{[Zn^{2+}]} = \frac{0.36M}{0.09M} = 4$$

Experiment 7:

4M NaOH; V_{NaOH}: 30mL

$M = \frac{n}{V} 4M = \frac{n}{0.030L} n_{NaOH} = 0.12$mol

1M$ZnCl_2$; V_{ZnCl_2}: 20mL

$M = \frac{n}{V} 1M = \frac{n}{0.02L} n_{ZnCl_2} = 0.02$mol

V_{total}= V_{NaOH} + V_{ZnCl_2}+ $V_{additive}$+ V_{water}= 30mL+20mL+5mL+45mL = 100mL

$[OH^-]$= $\frac{0.12mol}{0.100L} [OH^-] = 1.2$M

$[Zn^{2+}]$= $\frac{0.02mol}{0.100L} [Zn^{2+}] = 0.2$M

$$\frac{[OH^-]}{[Zn^{2+}]} = \frac{1.2M}{0.2M} = 6$$

Experiment 8:

4M NaOH; V_{NaOH}: 30mL

$M = \frac{n}{V} 4M = \frac{n}{0.030L} n_{NaOH} = 0.12\text{mol}$

1M$ZnCl_2$; V_{ZnCl_2}: 20mL

$M = \frac{n}{V} 1M = \frac{n}{0.02L} n_{ZnCl_2} = 0.02\text{mol}$

$V_{total} = V_{NaOH} + V_{ZnCl_2} + V_{additive} + V_{water}$ = 30mL+20mL+5mL+45mL = 100mL

$[OH^-] = \frac{0.12mol}{0.100L} [OH^-] = 1.2\text{M}$

$[Zn^{2+}] = \frac{0.02mol}{0.100L} [Zn^{2+}] = 0.2\text{M}$

$$\frac{[OH^-]}{[Zn^{2+}]} = \frac{1.2M}{0.2M} = 6$$

APPENDIX B

Calculation of Scherrer's Equation

XRD peaks are used for calculation of Scherrer's Equation. The highest intensity peaks take consideration for each XRD figure.

The XRD graph for Experiment 2 is given in Figure A.1 with drawing 2θ (degree) ,θ(degree) and intensity values.

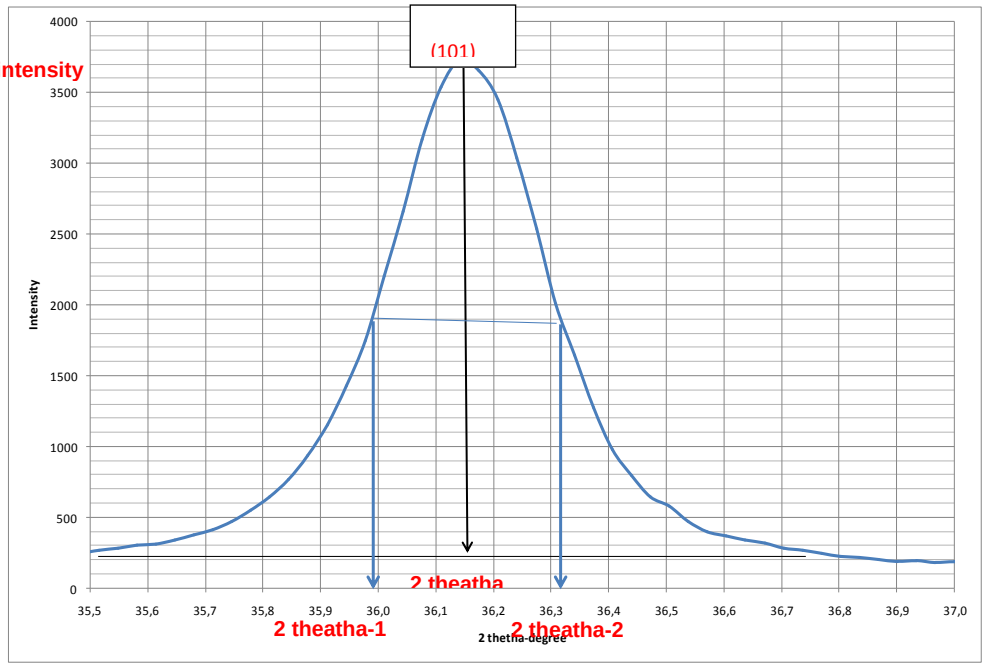

A.1. The 2θ (degree) ,θ(degree) and intensity values on XRD graph of Experiment 2

From Figure A.1, 2θ (degree) ,θ(degree) and intensity is determined. The full width is obtained to calculate the grain size diameter.

2θ (degree): 36,15

θ(degree): 18.075

Intensity: 3750

The Full Width at Half Maximum (FWHM):

(FWHM) = 36.32-35.11=0.33

B(radian) = (FWHM*3.14)/180 = 0.00576

Beta(radian) = $(B^2 - 0.00112^2)^{0.5}$ = 0.00565

D(A) = 0.9*1.5418/Beta(radian)/ COS((θ*3.14)/180)

D(A) = 258.3619

D(nm) = D(A) /10 = **25.84**

APPENDIX C

Band Gap Energy Calculations

Band Gap Energy is calculated from reflectance data by using Kubelka – Munk function.

$R_\infty = R / 100$

$F(R_\infty) \equiv (1 - R_\infty)^2 / 2R_\infty$

$[F(R_\infty)h\nu]^2$ is plotted against the $h\nu$ using the Kubelka-Munk function, where h is Plank's constant and ν is frequency of vibration. $h\nu$ is electron volts (eV) and its relationship to the wavelength λ (nm) is calculated.

$h\nu = 1240/\lambda$

$[F(R_\infty)h\nu]^2$ versus $h\nu$ is plotted for Experiment 2 and given in Figure B.1.

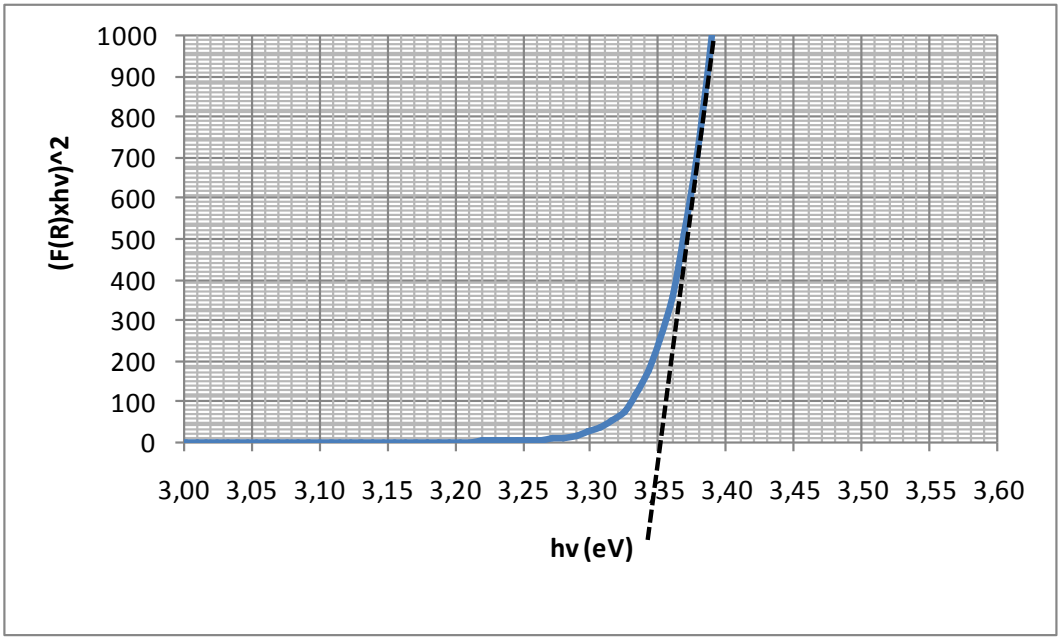

Figure B.1 $[F(R_\infty)h\nu]^2$ versus $h\nu$ for Experiment 2